

1 **Temporal inventory of glaciers in the Suru sub-basin, western**  
2 **Himalaya: Impacts of the regional climate variability**

3  
4 Aparna Shukla<sup>1,2\*</sup>, Siddhi Garg<sup>1</sup>, Manish Mehta<sup>1</sup>, Vinit Kumar<sup>1</sup>, Uma Kant Shukla<sup>3</sup>

5  
6 <sup>1</sup>Wadia Institute of Himalayan Geology, 33, GMS Road, Dehradun-248001, India

7 <sup>2</sup>Ministry of Earth Sciences, New Delhi– 110003, India

8 <sup>3</sup>Department of Geology, Banaras Hindu University, Varanasi –221005, India

9  
10 *\*Correspondence to:* Aparna Shukla (aparna.shukla22@gmail.com)

11  
12  
13  
14  
15  
16  
17  
18  
19  
20  
21  
22  
23  
24  
25  
26  
27  
28  
29  
30  
31  
32  
33  
34  
35  
36  
37  
38  
39  
40  
41

## 42 **Abstract**

43 Updated knowledge about the glacier extent and characteristics in the Himalaya cannot be overemphasised.  
44 Availability of precise glacier inventories in the latitudinally diverse western Himalayan region is particularly  
45 crucial. In this study we have created an inventory of the Suru sub-basin, western Himalaya for year 2017 using  
46 Landsat OLI data. Changes in glacier parameters have also been monitored from 1971 to 2017 using temporal  
47 satellite remote sensing data and limited field observations. Inventory data show that the sub-basin has 252  
48 glaciers covering 11% of the basin, having an average slope of  $25 \pm 6^\circ$  and dominantly north orientation. The  
49 average snow line altitude (SLA) of the basin is  $5011 \pm 54$  masl with smaller (47%) and cleaner (43%) glaciers  
50 occupying the bulk area. Longterm climate data (1901-2017) show an increase in the mean annual temperature  
51 ( $T_{\max}$  &  $T_{\min}$ ) by  $0.77^\circ\text{C}$  ( $0.25$  &  $1.3^\circ\text{C}$ ) in the sub-basin, driving the overall glacier variability in the region.  
52 Temporal analysis reveals a glacier shrinkage of  $\sim 6 \pm 0.02\%$ , an average retreat rate of  $4.3 \pm 1.02 \text{ ma}^{-1}$ , debris  
53 increase of 62% and  $22 \pm 60$  m SLA rise in past 46 years. This confirms their transitional response between the  
54 Karakoram and the Greater Himalayan Range (GHR) glaciers. Besides, glaciers in the sub-basin occupy two  
55 major ranges, i.e., GHR and Ladakh range (LR) and experience local climate variability, with the GHR glaciers  
56 exhibiting a warmer and wetter climate as compared to the LR glaciers. This variability manifestes itself in the  
57 varied response of GHR and LR glaciers. While the GHR glaciers exhibit an overall rise in SLA (GHR:  $49 \pm 69$   
58 m; LR: decrease by  $18 \pm 50$  m), the LR glaciers have deglaciated more (LR: 7%; GHR: 6%) with an enhanced  
59 accumulation of debris cover (LR: 73%; GHR: 59%). Inferences from this study reveal prevalence of glacier  
60 disintegration and overall degeneration, transition of clean ice to partially debris covered glaciers, local climate  
61 variability and non-climatic (topographic and morphometric) factor induced heterogeinty in glacier response as  
62 the major processes operatives in this region. The dataset Shukla et al., (2019) is accessible at  
63 <https://doi.pangaea.de/10.1594/PANGAEA.904131>

64  
65 **Key words:** Suru sub basin, western Himalaya, glacier inventory, climate change

66  
67 **Location of the dataset:** <https://doi.pangaea.de/10.1594/PANGAEA.904131>

## 69 **1 Introduction**

70 State of the Himalayan cryosphere has a bearing on multiple aspects of hydrology, climatology, environment  
71 and sustenance of living organisms at large (Immerzeel et al., 2010; Miller et al., 2012). Being sensitive to the  
72 ongoing climate fluctutations, glaciers keep adjusting themselves and these adaptations record the changing  
73 patterns in the global climate (Bolch et al., 2012). Any alteration in the glacier parameters would ultimately  
74 affect the hydrology of the region, thereby influencing the downstream communities (Kaser et al., 2010;  
75 Pritchard, 2017). Owing to these reasons, quantifying the mass loss over different Himalayan regions in the past  
76 years, ascertaining present status of the cryosphere and how these changes are likely to affect the freshwater  
77 accessibility in the region are at the forefront of contemporary cryospheric research (Brun et al. 2017; Sakai and  
78 Fujita, 2017). This aptly triggered several regional (Kaab et al., 2012; Gardelle et al., 2013; Brun et al. 2017;  
79 Zhou et al., 2018; Maurer et al., 2019) , local (Bhushan et al., 2018; Vijay and Braun, 2018) and glacier specific  
80 studies (Dobhal et al., 2013; Bhattacharya et al., 2016; Azam et al., 2018) in the region. These studies at varying

81 scales contribute towards solving the jigsaw puzzle of the Himalayan cryosphere. The regional scale studies  
82 operate on small scale for bringing out more comprehensive, holistic and synoptic spatio-temporal patterns of  
83 glacier response, the local scale studies monitor glaciers at basin level or groups and offer more details on  
84 heterogenous behaviour and plausible reasons thereof. However, the glacier specific studies whether based on  
85 field or satellite or integrative information are magnified versions of the local scale studies and hold the  
86 potential to provide valuable insights into various morphological, topographic and local-climate induced  
87 controls on glacier evolution. Despite these efforts, data on the glacier variability and response remain  
88 incomplete, knowledge of the governing processes still preliminary and the future viability pathways of the  
89 Himalayan cryospheric components are uncertain.

90 Though the literature suggests a generalised mass loss scenario (except for the Karakoram region) over the  
91 Himalayan glaciers, disparities in rates and pace of shrinkage remain. Maurer et al. (2019) report the average  
92 mass wastage of  $-0.32 \text{ m w.e.a}^{-1}$  for the Himalayan glaciers during 1975-2016. They suggest that the glaciers in  
93 the eastern Himalaya ( $-0.46 \text{ m w.e.a}^{-1}$ ) have experienced slightly higher mass loss as compared to the western ( $-$   
94  $0.45 \text{ m w.e.a}^{-1}$ ), followed by the central ( $-0.38 \text{ m w.e.a}^{-1}$ ). However, considerable variability in the glacier  
95 behaviour exists within the western Himalayas (Scherler et al., 2011; Kaab et al., 2012; Vijay and Braun, 2017;  
96 Bhushan et al., 2018; Mölg et al., 2018). Studies suggest that largely the glaciers in the Karakoram Himalayas  
97 have either remained stable or gained mass in the last few decades (Kääb et al., 2015; Cogley, 2016), while a  
98 contrasting behaviour is observed for the GHR glaciers experiencing large scale degeneration, with more than  
99 65% glaciers retreating during 2000-2008 (Scherler et al., 2011). However, there are two views pertaining to the  
100 glaciers in the Trans Himalayan range, with one suggesting their intermediate response between the Karakoram  
101 Himalaya and GHR (Chudley et al., 2017) and the other emphasizing upon their affinity either towards the GHR  
102 or the Karakoram Himalayan glaciers (Schmidt and Nusser, 2017). Therefore, in order to add more data and  
103 build a complete understanding of the glacier response, particularly in the western Himalaya, more local scale  
104 studies are necessary.

105 Complete and precise glacier inventories form the basic prerequisites not only for comprehensive glacier  
106 assessment but also for various hydrological and climate modelling related applications (Vaughan et al., 2013).  
107 Information on spatial coverage of glaciers in any region is a much valued dataset and holds paramount  
108 importance in the future assessment of glaciers. Errors in the glacier outlines may propagate and introduce  
109 higher uncertainties in the modelled outputs (Paul et al., 2017). Besides, results from modelling studies  
110 conducted over same region but using different sources of glacier boundaries are rendered uncomparable,  
111 constraining the evaluation of models and thus their future development. On the other hand, quality, accuracy  
112 and precision associated with glacier mapping and outline delineation requires dedicated efforts. Several past  
113 studies discuss the methods for, challenges in achieving an accurate glacier inventory and resolutions for the  
114 same (Paul et al., 2013; 2015; 2017). Thorough knowledge of glaciology and committed manual endeavour are  
115 two vital requirements in this regard. Realisation of above facts did result in several devoted attempts to prepare  
116 detailed glacier inventories at global scale, such as Randolph glacier inventory (RGI), Global land ice  
117 measurements from space (GLIMS) and recently Chinese glacier inventory (CGI) and Glacier area mapping for  
118 discharge from the Asian mountains (GAMDAM) (Raup et al., 2007; Pfeffer et al., 2014; Shiyin et al., 2014;  
119 Nuimura et al., 2015). However, several issues related to gap areas, differences in mapping methods and skills  
120 of the analysts involved act as limitations and need further attention.

121 Considering the above, present work studies the glaciers in the Suru Sub-basin (SSB), western Himalaya,  
122 Jammu and Kashmir. Primary objectives of this study include: 1) presenting the inventory of recent glacier data  
123 [area, length, debris cover, SLA, elevation (min & max), slope and aspect] in the SSB; 2) assessing the temporal  
124 changes for four epochs in past 46 years; and 3) analysing the observed glacier response in relation to the  
125 regional climate trends, local climate variability and other factors (regional hypsometry, topographic  
126 characteristics, debris cover and geomorphic features). Several remote sensing and field based studies of  
127 regional (Vijay and Braun, 2018) , local (Bhushan et al., 2018, Kamp et al., 2011; Pandey et al., 2011; Shukla  
128 and Qadir, 2016, Rashid et al 2017, Murtaza and Romshoo, 2015) and glacier-specific nature (Garg et al., 2018;  
129 2019; Shukla et al., 2018) have been conducted for monitoring the response of the glaciers to the climate  
130 change. Glaciological studies carried out in or adjacent to the SSB suggest increased shrinkage, slowdown and  
131 downwasting of the studied glaciers at variable rates (Kamp et al., 2011; Pandey et al., 2011; Shukla and Qadir,  
132 2016; Bhushan et al., 2018). These studies also hint towards the possible role of topographic & morphometric  
133 factors as well as debris cover in glacier evolution, though confined to their own specific regions. Previous  
134 studies have also estimated the glacier statistics of SSB and reported the total number of glaciers and the  
135 glacierized area to be 284 and 718.86 km<sup>2</sup> (Sangewar and Shukla, 2009) and 110 and 156.61 km<sup>2</sup> (SAC report,  
136 2016), respectively. While the RGI reports varying results by two groups of analysts (number of glaciers: 514 &  
137 304 covering an area of 550 & 606 km<sup>2</sup>, respectively) for 2000 itself.

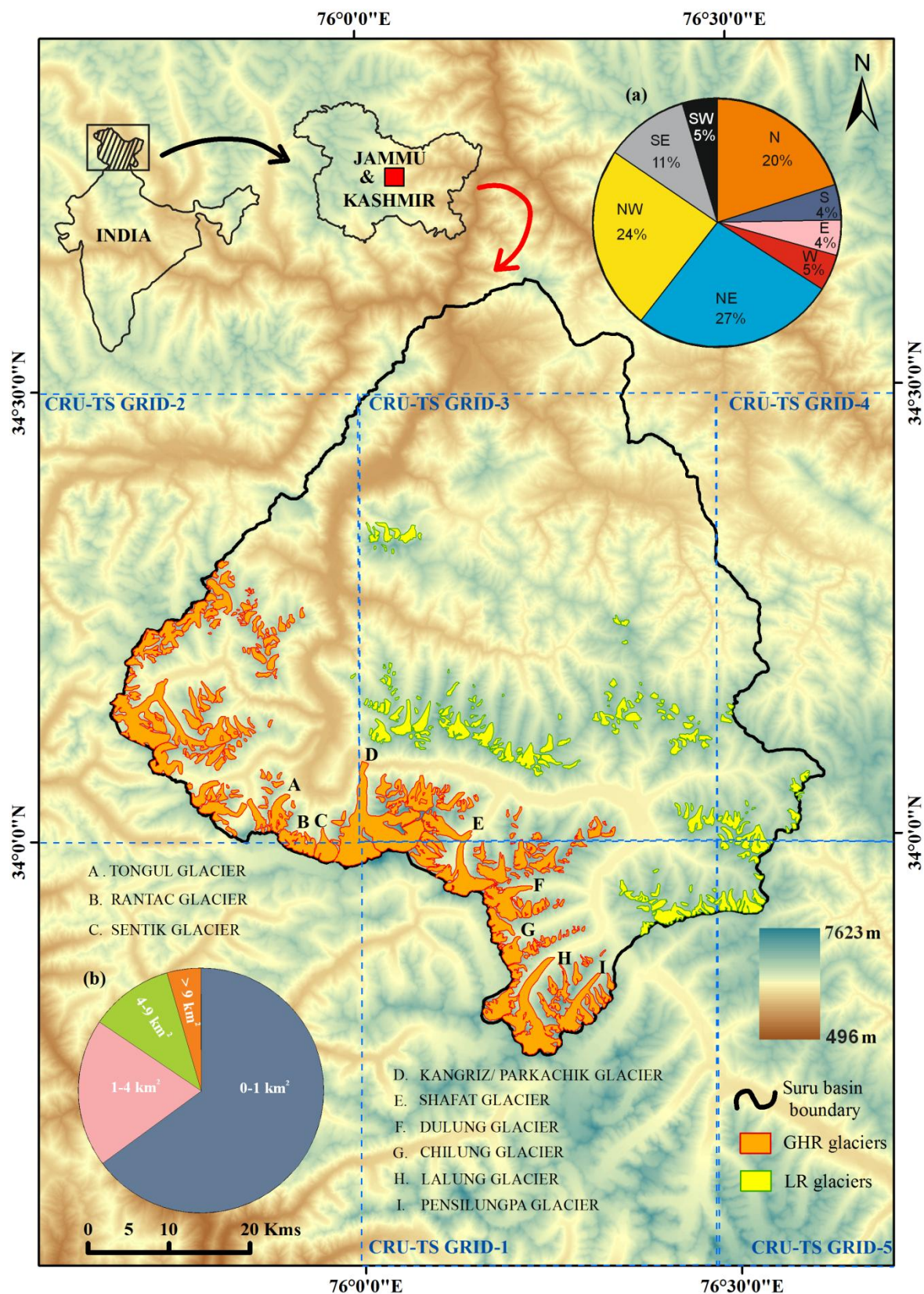
138 Previous findings suggesting progressive degeneration of glaciers, apparent variation and discrepancies in  
139 inventory estimates and also the fact that the currently available glacier details for the sub-basin are nearly 20  
140 years old, mandate the recent and accurate assessment of the glaciers in the SSB and drive the present study.

141

## 142 **2 Study area**

143 The present study focuses on the glaciers of the SSB situated in the state of Jammu and Kashmir, western  
144 Himalaya (Fig. 1). The geographic extent of the study area lies within latitude and longitude of 33° 50' to 34°  
145 40' N to 75° 40'to 76° 30' E.

146 Geographically, the sub-basin covers part of two major ranges, i.e., GHR and LR and shows the presence of the  
147 highest peaks of Nun (7135 masl) and Kun (7077 masl) in the GHR (Vittoz, 1954). The glaciers in these ranges  
148 have distinct morphology, with the larger ones located in the GHR and comparatively smaller towards the LR  
149 (Fig. 1).



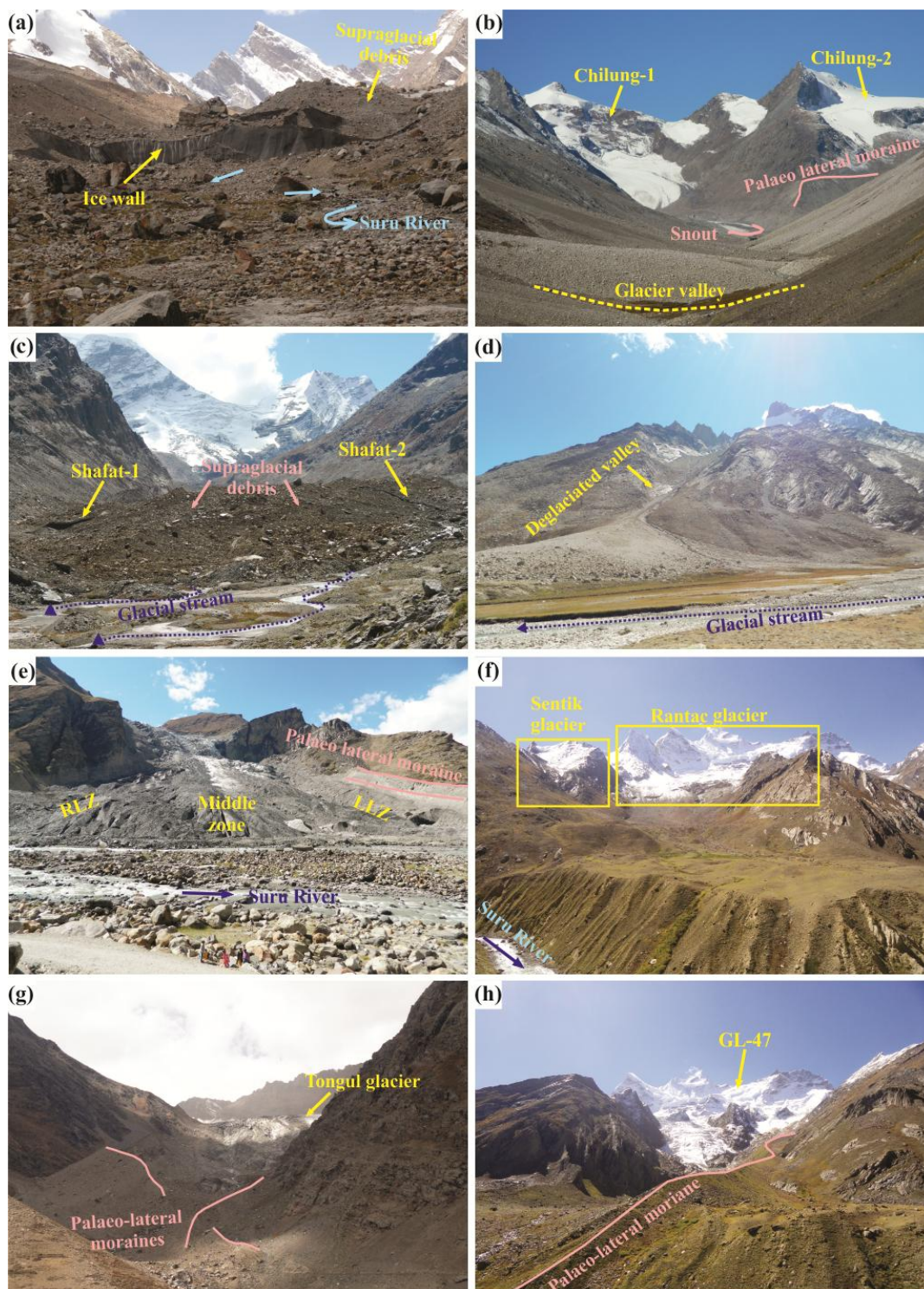
150

151 Figure 1: Location map of the study area. The glaciers in the Suru Sub-basin (black outline) are studied for their  
 152 response towards the climatic conditions during the period 1971-2017. Blue rectangles with dashed outlines  
 153 (GRID-1, 2, 3, 4 and 5) are the Climate Research Unit (CRU)-Time Series (TS) 4.02 grids of dimension 0.5° x  
 154 0.5°. (a) Pie-chart inset showing orientation-wise percentage distribution of glaciers in the sub-basin. North (N),  
 155 north-east (NE), north-west (NW), south (S), south-east (SE), south-west (SW), east (E) and west (W)

156 represents the direction of the glaciers. (b) Pie chart inset showing size-distribution of glaciers in the SSB. The  
157 glacier boundaries [GHR (orange) and LR (yellow)] are overlain on the Advanced Land Observing Satellite  
158 (ALOS) Digital Surface Model (DSM).

159

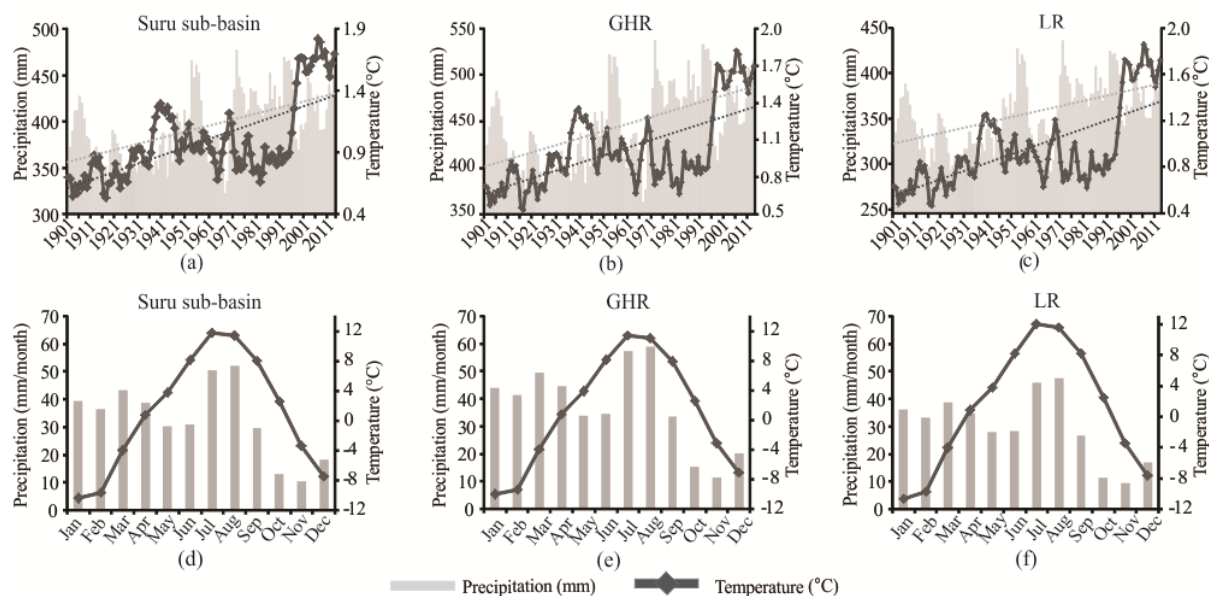
160 The meltwater from these glaciers feeds the Suru River (tributary of Indus River), which emerges from the  
161 Pensilungpa glacier (Fig. 2a) at an altitude of ~4675 m asl. The river further flows north for a distance of ~24  
162 kms and takes a westward turn from Rangdum (~4200 m asl). While flowing through this path, the Suru River is  
163 fed by some of the major glaciers of the GHR namely Lalung, Dulung (Fig. 1), Chilung (Fig. 2b), Shafat (Fig.  
164 2c; d), Kangriz/ Parkachik (Fig. 2e), Sentik, Rantac (Fig.2f), Tongul (Fig. 2g) and Glacier no.47 (Fig. 2h).  
165 Amongst these major glaciers, Kangriz forms the largest glacier in the SSB, covering an area of ~53 km<sup>2</sup> and  
166 descends down from the peaks of Nun and Kun (Garg et al., 2018). The Suru River continues to flow for a  
167 distance of nearly 54 kms and after crossing a mountain spur and the townships of Tongul, Panikhar and  
168 Sankoo, the river further flows north until it finally merges with River Indus at Nurla (~3028 m asl).



169  
 170 Figure 2: Field photographs of some of the investigated glaciers in the study area captured during the field visits  
 171 in September, 2016 and 2017. (a), (b), (c), (e), (f), (g), (h) Snouts of Pensilungpa, Chilung, Shafat, Kangriz,  
 172 Sentik & Rantac, Tongul glaciers and Glacier no.47, respectively. (d) Deglaciaded valley near the Shafat glacier.  
 173

174 The westerlies are an important source of moisture in this region (Dimri, 2013) with wide range of fluctuations  
 175 in snowfall during winters. In the Padum valley, annual mean precipitation (Snowfall) and temperature amounts  
 176 to nearly 2050 to 6840 mm and 4.3 °C, respectively (Raina and Kaul, 2011; <http://en.climate-data.org>). The  
 177 longterm average annual temperature and precipitation have varied from 5.5 °C/ 588.77 mm (Kargil) to -2.04

178 °C/ 278.65 mm in Leh during the period 1901-2002 (IMD, 2015). However, in order to understand the long term  
 179 variability of climatic conditions in the SSB, we have utilized the Climate Research Unit (CRU)-Time Series  
 180 (TS) 4.02 data during the period 1901-2017 (Fig. 3; Harris and Jones, 2018). Derived from this data, the annual  
 181 mean temperature and precipitation of the SSB for the period 1901-2017 has been  $0.99 \pm 0.45$  °C and  $393 \pm 76$   
 182 mm, respectively. (Standard deviations associated with the mean temperature and precipitation have been  
 183 italicized throughout the text).



184  
 185 Figure 3: Annual and seasonal variability in the climate data for the period 1901-2017. (a), (b) and (c) 5 year  
 186 moving average of the mean annual precipitation (mm) and temperature (°C) recorded for 5 grids covering the  
 187 glaciers in the entire SSB, GHR and LR (sub-regions), respectively during the period 1901-2017. The light and  
 188 dark grey colored dashed lines depict the respective trend lines for precipitation and temperature conditions  
 189 during the period 1901-2017. (d), (e) and (f) Monthly mean precipitation and temperature data for the entire  
 190 SSB, GHR and LR (sub-regions), respectively for the time period 1901-2017.

191

## 192 3 Datasets and Methods

### 193 3.1 Datasets used

194 The study uses multi-sensor and multi-temporal satellite remote sensing data for extracting the glacier  
 195 parameters for four time periods, i.e., 1971/1977, 1994, 2000 and 2017, details of which are mentioned in Table  
 196 1. It involves 6 Landsat level 1 terrain corrected (L1T), 3 strips of declassified Corona KH-4B and 1 Sentinel  
 197 multispectral scenes, downloaded from USGS Earth Explorer (<https://earthexplorer.usgs.gov/>). Besides, a global  
 198 digital surface model (DSM) dataset utilizing the data acquired by the Panchromatic remote-sensing Instrument  
 199 for Stereo Mapping (PRISM) onboard the Advanced Land Observing Satellite (ALOS) have also been  
 200 incorporated (<https://www.eorc.jaxa.jp/ALOS/en/aw3d30/>). ALOS World 3D comprises of a fine resolution  
 201 DSM (approx 5m vertical accuracy). It is primarily used for delineating the basin boundary, extraction of SLA,  
 202 elevation range, regional hypsometry and slope.

203

204 Table 1: Detailed specifications of the satellite data utilised in the present study. GB= glacier boundaries,  
 205 DC=debris cover



S. no	Satellite sensors(Date of acquisition)	Remarks on quality	Scene Id	RMSE error	Registration accuracy (m)	Purpose
1.	Corona KH-4B (28 Sep 1971)	Cloud free	DS1115-2282DA056/ DS1115-2282DA055/ DS1115-2282DA054	0.1	0.3	Delineation of GB
2.	LandsatMSS (19 Aug 1977/ 1 Aug 1977)	Cloud free/ peak ablation (17 Aug)	LM02_L1TP_159036_19770819_20180422_01_T2/ LM02_L1TP_159036_19770801_20180422_01_T2	0.12	10	Delineation of GB, SLA&DC
3.	LandsatTM (27 Aug 1994)	Partially cloud covered/ peak ablation	LT05_L1TP_148036_19940827_20170113_01_T1/ LT05_L1GS_148037_19940827_20170113_01_T2	0.22	6	Delineation of GB, SLA&DC
4.	LandsatTM (26 July 1994)	Seasonal snow cover	LT05_L1TP_148036_19940726_20170113_01_T1	0.2	6	Delineation of GB
5.	LandsatET M <sup>+</sup> (4 Sep 2000)	Cloud free/ peak ablation	LE71480362000248S GS00	Base image		Delineation of GB, SLA&DC
6.	LandsatOLI (25July 2017)	Partially cloud covered/ peak ablation	LC08_L1TP_148036_20170810_01_T1	0.15	4.5	Delineation of GB & DC, estimation of SLA
7.	Sentinel MSI (20 Sep 2017)	Cloud free	S2A_MSIL1C_20170920T053641_N0205_R005_T43SET_20170920T053854	0.12	1.2	Delineation of GB & DC
8.	LISS IV (27Aug2017)	Cloud free	183599611	0.2	1.16	Accuracy assessment

207 The aforementioned satellite images were acquired keeping into consideration certain necessary pre-requisites,  
208 such as, peak ablation months (July/ August/ September), regional coverage, minimal snow and cloud cover for  
209 the accurate identification and demarcation of the glaciers. Only three Corona KH-4B strips were available for  
210 period 1971, which covered the SSB partially, i.e., 40% of the GHR and 57% of the LR glaciers. Therefore, rest  
211 of the glaciers were delineated using the Landsat MSS image of the year 1977 (Table 1). Similarly, some of the  
212 glaciers could not be mapped using the Landsat TM image of 27 Aug 1994 as the image was partially covered  
213 with clouds. Therefore, 26 July 1994 image of the same sensor was used in order to delineate the boundaries of  
214 the cloud covered glaciers.

215 Besides, long term climate data have been obtained from CRU-TS 4.02, which is a high resolution gridded  
216 climate dataset obtained from the monthly meteorological observations collected at different weather stations of  
217 the World. In order to generate this long term data, station anomalies from 1961-1990 are interpolated into  $0.5^\circ$   
218 latitude and longitude grid cells (Harris and Jones, 2018). This dataset includes six independent climate  
219 variables (mean temperature, diurnal temperature range, precipitation, wet-day frequency, vapour pressure and  
220 cloud cover). However, in this study monthly mean, minimum and maximum temperature and precipitation data  
221 are taken into consideration.

222

## 223 **3.2 Methodology adopted**

224 The following section mentions the methods adopted for data extraction, analysis and uncertainty estimation.

225

### 226 **3.2.1 Glacier mapping and estimation of glacier parameters**

227 Initially, the satellite images were co-registered by projective transformation at sub-pixel accuracy with the  
228 Root Mean Square Error (RMSE) of less than 1m (Table 1), taking the Landsat ETM<sup>+</sup> image and ALOS DSM  
229 as reference. However, the Corona image was co-registered following a two step approach: (1) projective  
230 transformation was performed using nearly 160-250 GCPs (2) spline adjustment of the image strips (Bhambri et  
231 al., 2012). The glaciers were mapped using a hybrid approach, i.e., normalized difference snow index (NDSI)  
232 for delineating snow-ice boundaries and manual digitization of the debris cover. Considering that not many  
233 changes would have occurred in the accumulation region, major modifications have been done in the boundaries  
234 below the equilibrium line altitude (ELA) (Paul et al., 2017). The glacierets/ tributary glaciers contributing to  
235 the main trunk are considered as single glacier entity. NDSI was applied on a reference image of Landsat ETM<sup>+</sup>  
236 using an area threshold range of 0.55-0.6. A median filter of kernel size 3\*3 was used to remove the noise and  
237 very small pixels. In this manner, glaciers covering a minimum area of 0.01 km<sup>2</sup> have been mapped. However,  
238 some pixels of frozen water, shadowed regions were manually corrected. Thereafter, the debris covered part of  
239 the glaciers was mapped manually by taking help from slope and thermal characteristics of the glaciers. Besides,  
240 high resolution imageries from the Google Earth<sup>TM</sup> were also referred for the accurate demarcation of the  
241 glaciers. Identification of the glacier terminus was done based on the presence of certain characteristic features  
242 at the snout such as ice wall, proglacial lakes and emergence of streams. Length of the glacier was measured  
243 along the central flow line (CFL) drawn from the bergschrund to the snout. Fluctuations in the snout position  
244 (i.e., retreat) of an individual glacier was estimated using the parallel line method, in which parallel strips of 50  
245 m spacing are taken on both sides of the CFL. Thereafter, the average values of these strips intersecting the  
246 glacier boundaries were used to determine the frontal retreat of the glaciers (Shukla and Qadir, 2016; Garg et al.,

247 2017a;b). Mean SLA estimated at the end of the ablation season can be effectively used as a reliable proxy for  
 248 mass balance estimation for a hydrological year (Guo et al., 2014). The maximum spectral contrast between  
 249 snow and ice in the SWIR and NIR bands helps in delineation of the snow line separating the two facies. The  
 250 same principle was used in this study to yield the snow line. Further, a 15 m sized buffer was created on both  
 251 sides of the snow line to obtain the mean SLA. Other factors such as elevation (max & min), regional  
 252 hypsometry and slope were extracted utilising the ALOS DSM.

253

### 254 3.2.2 Analysis of climate variables

255 To ascertain the long term climate trends in the sub-basin, mean annual temperature (min & max) and  
 256 precipitation are derived by averaging the mean monthly data of the respective years. Besides, seasonal trends  
 257 are also analysed for winter (November-March) and summer (April-October) months. Moreover, the climate  
 258 variables are assessed separately for the ~46 year period (1971-2017), which is the study period of present  
 259 research.

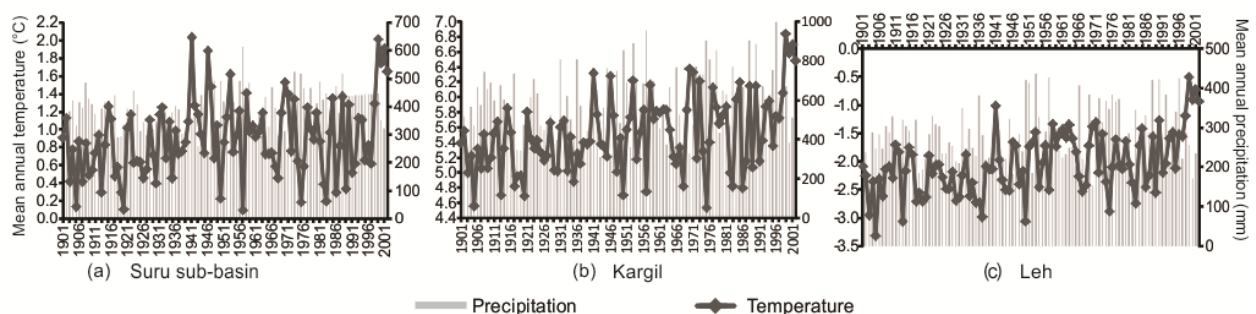
260 Further, the climate dataset was statistically analysed for five grids using Mann-Kendall test to obtain the  
 261 magnitude and significance of the trends (Supplementary table S2). The magnitude of trends in time series data  
 262 was determined using Sen's slope estimator (Sen, 1968). Quantitatively, the temperature and precipitation trends  
 263 have been assessed here in absolute terms (determined from Sen's slope). The change in climate parameters  
 264 (temperature and precipitation) was determined using following formula:

$$265 \text{ Change} = (\beta * L) / M \quad (1)$$

266 where  $\beta$  is Sen's slope estimator,  $L$  is length of period and  $M$  is the long term mean.

267 These tests were performed at confidence level,  $S = 0.1(90\%)$ ,  $0.05(95\%)$  and  $0.01(99\%)$ , which differed for  
 268 both the variables (Supplementary table S2). Spatial interpolation of climate data was achieved using the Inverse  
 269 Distance Weighted (IDW) algorithm. For this purpose, a total number of 15 CRU TS grids (in vicinity of our  
 270 study area) were taken so as to have an ample number of data points in order to achieve the accurate results.

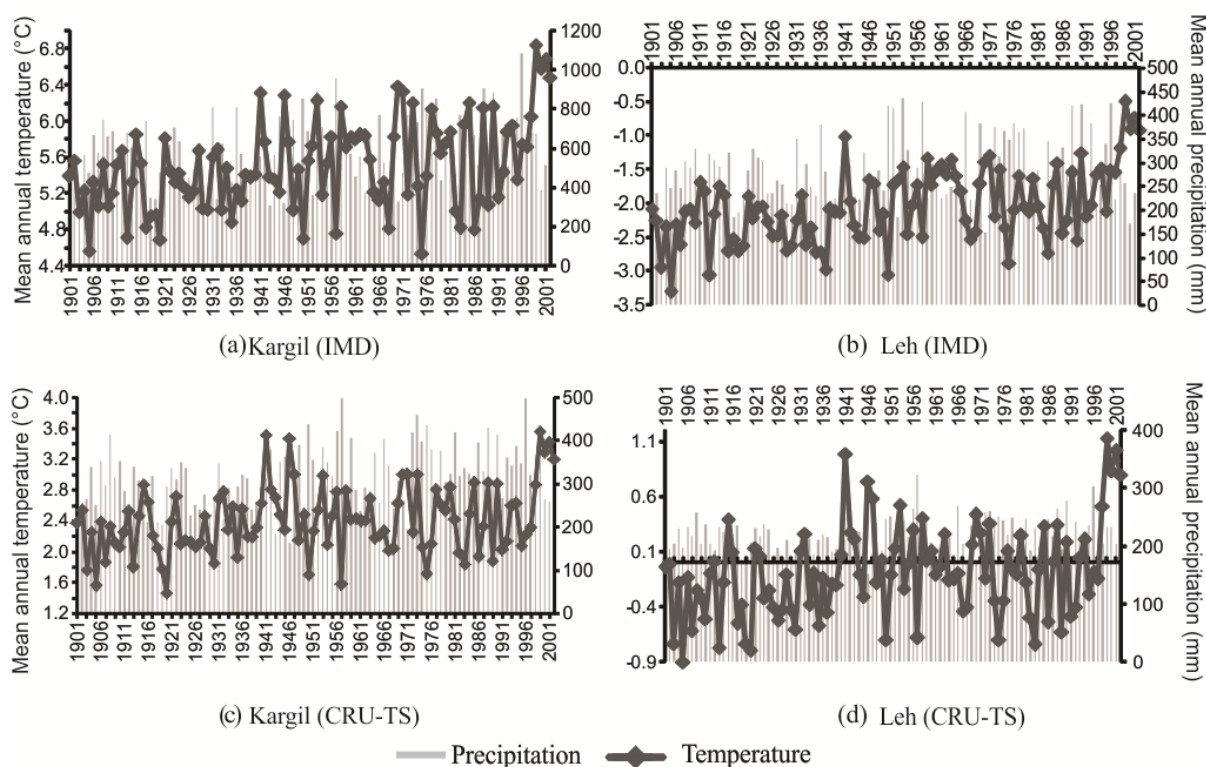
271 Further, in order to check data consistency, we have taken instrument data from nearest stations of Kargil and  
 272 Leh (due to the unavailability of meteorological stations in the Suru sub-basin) and compared with the CRU-TS  
 273 derived data for the entire Suru sub-basin during 1901-2002 period (Fig. 4).



274

275 Figure 4: Mean annual temperature and precipitation patterns of CRU-TS derived gridded data in (a) Suru sub-  
 276 basin and IMD recorded station at (b) Kargil and (c) Leh.

277 The mean annual temperature pattern of Suru sub-basin shows a near negative trend till 1937, with an increase  
 278 thereafter. Similar trends have been observed for Kargil and Leh, despite their distant location from the Suru  
 279 sub-basin (areal distance of Kargil and Leh is ~63 and 126 km, respectively from the centre of Suru sub-basin).  
 280 However, it is noteworthy to mention that all the locations had attained maximum mean annual temperature in  
 281 1999 (Suru: 2.02°C; Kargil: 6.84°C; Leh: -0.5°C). We observe an almost similar trend in all the cases (Fig. 4),  
 282 with an accelerated warming post 1995/96. However, the magnitude varies, with longterm mean annual  
 283 temperature of 0.9, 5.5 and -2.04°C observed in Suru sub-basin, Kargil and Leh, respectively (Fig. 4). The  
 284 possible reason for this difference in their magnitudes could possibly be attributed to their distinct geographical  
 285 locations and difference in their nature, with former being point, while latter being the interpolated gridded data.  
 286 Also, we have used the station data, obtained from nearest available IMD sites, i.e., Kargil and Leh and  
 287 compared with their respective CRU-TS data (mean annual temperature and precipitation).



288  
 289 Figure 5: Analysis of meteorological (mean annual temperature and precipitation) datasets derived from Indian  
 290 Meteorological Department (IMD) stations at (a) Kargil & (b) Leh and the respective [(c) Kargil and (d) Leh]  
 291 gridded data obtained from climate research unit (CRU)-time series (TS).

292 Though varying in magnitude, the climate data obtained from IMD as well as CRU-TS suggest almost similar  
 293 trends of temperature and precipitation during the period 1901-2002 for both Kargil and Leh (Fig. 5). The  
 294 annual mean temperature/ precipitation amounted to 5.5°C/589 mm (IMD) and 2.4°C/315 mm (CRU-TS) in  
 295 Kargil, while -2.04/279 mm (IMD) and -0.09/ 216 mm (CRU-TS) in Leh during the period 1901-2002 (Fig.  
 296 5). We observed that climatic variables show lower magnitude in case of CRU-TS as compared to the station  
 297 data from IMD (except CRU-TS derived temperature data recorded for Leh). The possible reason for this  
 298 difference between CRU-TS and station data can primarily be attributed to the difference in their nature, with  
 299 former being point, while latter being a gridded data (0.5° latitude and longitude grid cells). This analysis aptly

300 brings out the bias in the CRU TS gridded data. Majorly the comparison shows that though the gridded data  
 301 correctly bring out the temporal trends in meteorological data, but differ with station data in magnitude (being  
 302 on lower side than the station estimates). This helps us better appreciate the climate variations in the Suru sub-  
 303 basin as well, since we learn that the reported temperature and precipitation changes are probably on the lower  
 304 side of the actual variations.

### 305 3.2.3 Uncertainty assessment

306 This study involves extraction of various glacial parameters utilizing satellite data with variable characteristics,  
 307 hence, susceptible to uncertainties, which may arise from various sources. These sources may be locational  
 308 (LE), interpretational (IE), classification (CE) or processing (PE) errors (Racoviteanu et al., 2009; Shukla and  
 309 Qadir, 2016). In our study, the LE and PE may have resulted on account of miss-registration of the satellite  
 310 images and inaccurate mapping, respectively. While IE and CE would have introduced due to the miss-  
 311 interpretation of glacier features during mapping. The former can be rectified by co-registration of the images  
 312 and estimation of sub-pixel co-registration RMSE (Table 1) and using standard statistical measures. However,  
 313 the latter can be visually identified and corrected but difficult for exact quantification owing to lack of reliable  
 314 reference data (field data) in most cases. As a standard procedure for uncertainty estimation, glacier outlines are  
 315 compared directly with the ground truth data as acquired using a Differential Global Positioning System (DGPS)  
 316 (Racoviteanu et al., 2008a). In this study, DGPS survey was conducted on the Pensilungpa and Kangriz glaciers  
 317 at an error of less than 1cm. Therefore, by comparing the snout position of Pensilungpa (2017) and Kangriz  
 318 (2018) glaciers derived from DGPS and OLI image, an accuracy of  $\pm 23$  and  $\pm 1.4$  m, respectively was obtained.  
 319 Also, the frontal retreat estimated for the Kangriz glacier using DGPS and OLI image is found to be  $38.63 \pm 47.8$   
 320 and  $39.98 \pm 56.6$  m, respectively during the period 2017-18. In this study, high resolution Linear imaging self-  
 321 scanning system (LISS)-IV imagery (spatial resolution of 5.8 m) is also used for validating the glacier mapping  
 322 results for the year 2017 (Table 1). Glaciers of varying dimensions and distribution of debris cover were  
 323 selected for this purpose. The area and length mapping accuracy for these selected glacier boundaries (G-1, G-2,  
 324 G-3, G-13, G-41, G-209, G-215, G-216, G-220, G-233) was found to be 3% and 0.5%, respectively.  
 325 The multi-temporal datasets were assessed for glacier length and area change uncertainty as per the methods  
 326 given by Hall et al. (2003) and Granshaw and Fountain (2006). Following formulations (Hall et al., 2003) were  
 327 used for estimation of the said parameters:

$$328 \text{Terminus uncertainty } (U_T) = \sqrt{a^2 + b^2} + \sigma \quad (2)$$

329 where, 'a' and 'b' are the pixel resolution of image 1 and 2, respectively and ' $\sigma$ ' is the registration error. The  
 330 terminus and areal uncertainty estimated are given in Table 2.

$$331 \text{Area change uncertainty } (U_A) = 2 * U_T * x \quad (3)$$

332 where, 'x' is the spatial resolution of the sensor.

333 Table 2. Terminus and Area change uncertainty associated with satellite dataset as defined by Hall et al. (2003).  
 334  $U_T$ = terminus uncertainty,  $U_A$ = area change uncertainty, x= spatial resolution,  $\sigma$  = registration accuracy.

Serial no.	Satellite sensor	Terminus uncertainty $U_T$ $=\sqrt{a^2 + b^2} + \sigma$	Area change uncertainty $U_A = 2 U_T * x$
------------	------------------	--	--

1.	Corona KH-4B	3.12 m	0.00007 km <sup>2</sup>
2.	Landsat MSS	123.13 m	0.03km <sup>2</sup>
3.	Landsat TM	41.42 m	0.003 km <sup>2</sup>
4.	Landsat ETM <sup>+</sup>	48.42 m	0.003km <sup>2</sup>
5.	Landsat OLI	46.92 m	0.003km <sup>2</sup>

337

338

339

340

341

342

343

344

345

346

347

348

349

350

351

Area mapping uncertainty was estimated using the buffer method, in which, a buffer size equal the registration error of the satellite image was taken into consideration (Bolch et al., 2012; Garg et al., 2017a,b). Error estimated using this method is found to be 0.48, 27.2, 9.6 and 3.41 km<sup>2</sup> for the 1971 (Corona), 1977 (MSS), 1994 (TM) and 2017 (OLI) image, respectively. Since the debris extents were delineated within the respective glacier boundaries, the proportionate errors are likely to have propagated in debris cover estimations which were estimated accordingly (Garg et al., 2017b).

Uncertainty in SLA estimation needs to be reported in the X, Y and Z directions. In this context, error in X and Y directions should be equal to the distance taken for creating the buffer on either side of the snow line demarcating the snow and ice facies. Since, the buffer size taken in this study was 15 m, therefore, error in X and Y direction was considered as  $\pm 15$  m. However, uncertainty in Z direction would be similar to the ALOS DSM, i.e.,  $\pm 5$  m.

## 4 Results

352

353

354

355

356

The present study involved creation of glacier inventory for the year 2017 and estimation of glacier (area, length, debris cover and SLA) parameters for four different time periods. For detailed insight, the variability of the glacier parameters have also been evaluated on decadal scale, in which the total time period has been subdivided into three time frames, i.e., 1971-1994 (23 years), 1994-2000 (6 years) and 2000-2017 (17 years).

357

### 4.1 Basin statistics

358

359

360

361

362

363

The SSB covers an area of  $\sim 4429$  km<sup>2</sup>. In 1971, the sub-basin had around 240 glaciers, with 126 glaciers located in the GHR and 114 in the LR, which remained the same till 2000. However, a major disintegration of glaciers took place during the period 2000-2017, which resulted into the breakdown of about 12 glaciers into smaller glacierets. The recent (2017) distribution of the glaciers in the GHR and LR is 130 and 122, respectively (Supplementary table S1). The overall glacierized area is  $\sim 11\%$ , with the size and length of the glaciers varying from 0.01 to 53.1 km<sup>2</sup> and 0.15 to 16.34 km, respectively.

364

365

366

367

368

369

370

371

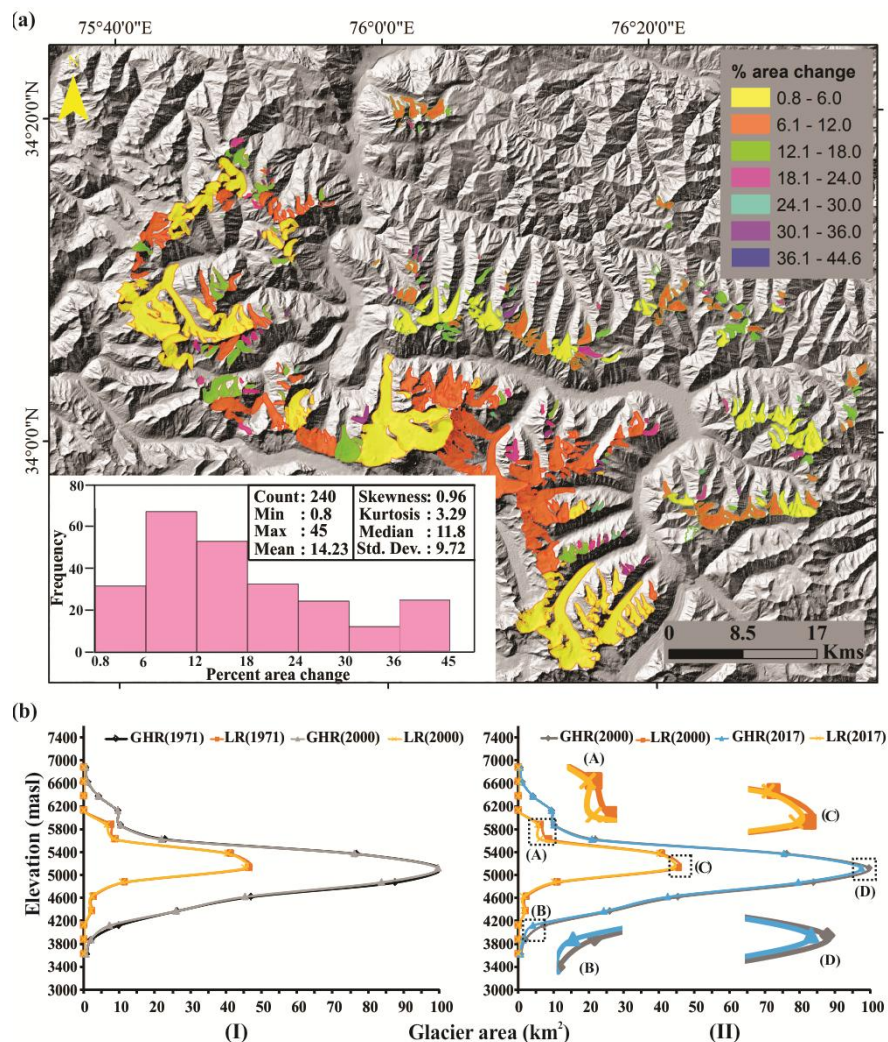
Within the sub-basin, the size range of glaciers in the GHR and LR vary from 0.01 (G-115) to 53.1 km<sup>2</sup> (G-50) and 0.03 (G-155/165) to 6.73 km<sup>2</sup> (G-209), respectively. Considering this, glaciers have been categorized into small (0-7 km<sup>2</sup>/ 0-2 km), medium (7-15 km<sup>2</sup>/ 2-7 km) and large (>15 km<sup>2</sup>/ >7 km). Based on size distribution, small (comprising all the LR and some GHR glaciers), medium and large glaciers occupy 47%, 15% and 38% of the glacierized sub-basin. Depending upon the percentage area occupied by the supraglacial debris out of the total glacier area, the glaciers have been categorized into clean (CG: 0-25%), partially debris-covered (PDG: 25-50%) and heavily debris-covered (HDG: >50%). Categorization of the glaciers based on this criteria shows their proportion in the glacierized basin as: CG (43%), PDG (40%) and HDG (17%). Majority of the glaciers in the

372 sub-basin are north facing (N/ NW/NE: 71%), followed by south (S/ SW/ SE: 20%), with very few oriented in  
 373 other (E/ W: 9%) directions (Fig. 1a). The mean elevation of the glaciers in the SSB is  $5134.8 \pm 225$  masl, with  
 374 an average elevation of  $5020 \pm 146$  and  $5260 \pm 117$  masl in the GHR and LR, respectively. Mean slope of the  
 375 glaciers is  $24.8 \pm 5.8^\circ$  and varies from  $24 \pm 6^\circ$  to  $25 \pm 6^\circ$  in the GHR and LR, respectively. While, percentage  
 376 distribution of glaciers shows that nearly 80% of the LR glaciers have steeper slope (20-40°) as compared to the  
 377 GHR glaciers (57%).

378

#### 379 4.2 Area changes

380 The glaciated area reduced from  $513 \pm 14$  km<sup>2</sup> (1971) to  $481 \pm 3.4$  km<sup>2</sup> (2017), exhibiting an overall deglaciation  
 381 of  $32 \pm 9$  km<sup>2</sup> ( $6 \pm 0.02\%$ ) during the period 1971-2017. Percentage area loss of the individual glaciers ranges  
 382 between 0.8 (G-50; Parkachik glacier) - 45 (G-81) %, with majority of the glaciers undergoing an area loss in  
 383 the range 6-12% during the period 1971-2017 (Fig.6a).



384

385 Figure 6: (a) Percent area loss of the glaciers in the SSB during the period 1971-2017. Frequency distribution  
 386 histogram depicting that majority of the glaciers have undergone an area loss in the range 6-12%. (b)  
 387 Hypsometric distribution of glacier area in the GHR and LR regions during the period (I) 1971-2000 and (II)  
 388 2000-2017. (A), (B), (C) and (D) insets in (II) shows the significant change in area at different elevation range  
 389 of the GHR and LR glaciers.

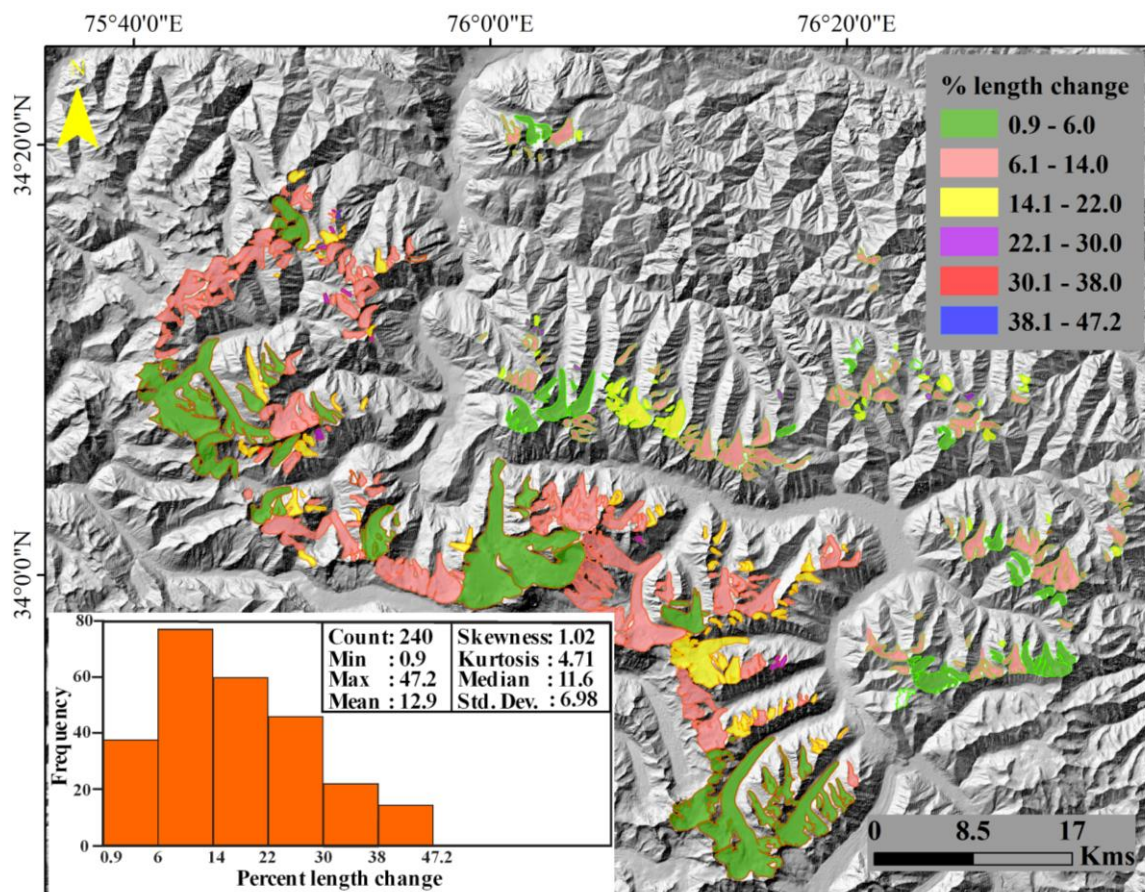
390

391 Results show that the highest pace of deglaciation is observed during 1994-2000 ( $0.95 \pm 0.005 \text{ km}^2\text{a}^{-1}$ ) and 2000-  
 392 2017 ( $0.86 \pm 0.0002 \text{ km}^2\text{a}^{-1}$ ) followed by 1971-1994 ( $0.5 \pm 0.001 \text{ km}^2\text{a}^{-1}$ ) (Supplementary figure S1a). Within the  
 393 SSB, glaciers in the LR exhibit higher deglaciation ( $7 \pm 7.2\%$ ) as compared to GHR ( $6 \pm 2\%$ ) during the period  
 394 1971-2017. Apart from deglaciation, G-50 also showed increment in glacier area during the period 1994-2000,  
 395 however, insignificantly.

396

### 397 4.3 Length changes

398 Fluctuations in the glacier snout have been estimated during the period 1971-2017 and it is observed that nearly  
 399 all the glaciers have retreated during the said period, however the retreat rates vary considerably. The overall  
 400 average retreat rate of the glaciers is observed to be  $4.3 \pm 1.02 \text{ ma}^{-1}$  during the period 1971-2017. Percentage  
 401 length change of the glaciers ranges between 0.9 to 47%, with majority of the glaciers retreating in the range 6-  
 402 14% during the period 1971-2017 (Fig.7).



403  
 404 Figure 7: Percent length change of the glaciers in the SSB during the period 1971-2017. Frequency distribution  
 405 histogram showing that majority of the glaciers have undergone length change of in the range 6-14%.  
 406

407 Decadal observations reveal the highest rate of retreat during 1994-2000 ( $7.37 \pm 8.6 \text{ ma}^{-1}$ ) followed by 2000-  
 408 2017 ( $4.66 \pm 1.04 \text{ ma}^{-1}$ ) and lowest during 1971-1994 ( $3.22 \pm 2.3 \text{ ma}^{-1}$ ) (Supplementary figure S 1b). Also, the  
 409 average retreat rate in the GHR and LR glaciers was observed to be  $5.4 \pm 1.04 \text{ ma}^{-1}$  and  $3.3 \pm 1.04 \text{ ma}^{-1}$ ,  
 410 respectively, during the period 1971-2017. The retreat rate of individual glaciers varied from  $0.72 \pm 1.02 \text{ ma}^{-1}$



411 (G-114) to  $28.92 \pm 1.02 \text{ ma}^{-1}$  (G-7, i.e., Dulung glacier) during the period 1971-2017. Besides, the Kangriz  
 412 glacier (G-50) also showed advancement during the period 1994-2000 by  $5.23 \pm 8.6 \text{ ma}^{-1}$ .

413

#### 414 **4.4 Debris-cover changes**

415 Results show an overall increase in debris-cover extent by 62% ( $\sim 37 \pm 0.002 \text{ km}^2$ ) in the SSB glaciers during the  
 416 period 1971-2017. Decadal variations exhibit the maximum increase in the debris-cover by approximately 19  
 417  $\pm 0.00004 \text{ km}^2$  (24%) during 2000-2017 followed by an increase of  $13 \pm 0.0001 \text{ km}^2$  (20%) and  $5 \pm 0.0001 \text{ km}^2$   
 418 (9%) during 1994-2000 and 1971-1994, respectively (Supplementary figure S1c). However, GHR and LR  
 419 glaciers show an overall increase of debris cover extent by 59% and 73%, respectively during the entire study  
 420 period, i.e., 1971-2017.

421

#### 422 **4.5 SLA variations**

423 The mean SLA shows an average increase of  $22 \pm 60 \text{ m}$  during the period 1977-2017. On the decadal scale, SLA  
 424 variations showed the highest increase ( $161 \pm 59 \text{ m}$ ) during 1994-2000 with a considerably lower increase ( $8 \pm 59$   
 425  $\text{m}$ ) during 1977-1994 and decrease ( $150 \pm 60 \text{ m}$ ) during 2000-2017. Amongst the four time periods (1977, 1994,  
 426 2000 & 2017) used for mean SLA estimation, the highest SLA is noted during 2000 ( $5158 \pm 65 \text{ masl}$ ) and  
 427 minimum during 1977 ( $4988 \pm 65 \text{ masl}$ ) (Supplementary figure S1d).

428 During the period 1977-2017, the average SLA of the LR glaciers is observed to be relatively higher ( $5155 \pm 7$   
 429  $\text{masl}$ ) as compared to the GHR glaciers ( $4962 \pm 9 \text{ masl}$ ). In contrast, an overall rise in mean SLA was noted in  
 430 GHR ( $49 \pm 69 \text{ m}$ ), while a decrease in LR glaciers ( $18 \pm 45 \text{ m}$ ) during the time frame of 1977-2017.

431

### 432 **5 Discussion**

433 The present study reports detailed temporal inventory data of the glaciers in the SSB considering multiple  
 434 glacier parameters, evaluates the ensuing changes for ascertaining the status of glaciers and relates them to  
 435 climate variability and other inherent terrain characteristics. The results suggest an overall degeneration of the  
 436 glaciers with pronounced spatial and temporal heterogeneity in response.

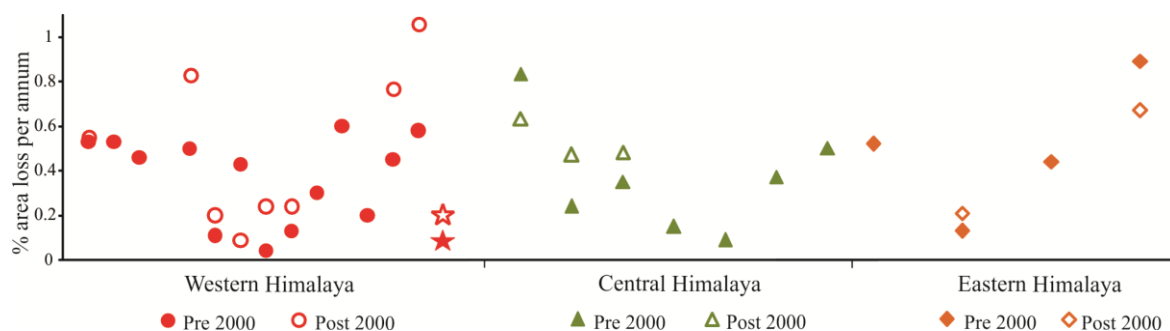
437

#### 438 **5.1 Glacier variability in Suru sub-basin: A comparative evaluation**

439 Basin statistics reveal that in the year 2000, the SSB comprised of 240 glaciers covering an area of  
 440 approximately  $496 \text{ km}^2$ . However, these figures differ considerably from the previously reported studies in this  
 441 particular sub-basin, with the total number of glaciers and the glacierized area varying from 284/  $718.86 \text{ km}^2$   
 442 (Sangewar and Shukla, 2009) to 110/  $156.61 \text{ km}^2$  (SAC report, 2016), respectively. In contrast, the glacierized  
 443 area is found to be less, however comparable with the RGI boundaries ( $550.88 \text{ km}^2$ ). Besides, debris cover  
 444 distribution of the glaciers during 2000 is observed to be  $\sim 16\%$  in the present study, which is almost half of that  
 445 reported in RGI (30%). Variability in these figures is possibly due to the differences in the mapping techniques,  
 446 thereby increasing the risk of systematic error. Moreover, due to the involvement of different analysts in the  
 447 latter, the results may more likely suffer with random errors.

448 Results from this study reveal an overall deglaciation of the glaciers in the SSB at an annual rate of  $\sim 0.1$   
 449  $\pm 0.0004\%$  during the period 1971-2017. This quantum of area loss is comparatively less to the average annual

450 rate of 0.4% reported in the western Himalaya (Supplementary table S3). However, our results are comparable  
 451 with Birajdar et al. (2014), Chand and Sharma (2015) and Patel et al. (2018) and differ considerably with other  
 452 studies in the western Himalayas (Supplementary table S3). Period wise deglaciation varied from  $0.1 \pm 0.0007$  to  
 453  $0.2 \pm 0.005\% \text{ a}^{-1}$  during 1971-2000 and 2000-2017, respectively. This result is in line with the recent findings by  
 454 Maurer et al. (2019), who suggest a higher average mass loss post 2000 ( $-0.43 \text{ m w.e.a}^{-1}$ ), which is almost  
 455 double the rate reported during 1975-2000 ( $-0.22 \text{ m w.e.a}^{-1}$ ) for the entire Himalaya.  
 456 Comparing the deglaciation rates of the glaciers within the western Himalayan region reveals considerable  
 457 heterogeneity therein (Supplementary table S3). It is observed that the Karakoram Himalayan glaciers, in  
 458 particular had been losing area till 2000 at an average rate of  $0.09\% \text{ a}^{-1}$ , with an increase in area thereafter by  
 459  $\sim 0.05\% \text{ a}^{-1}$  (Liu et al., 2006; Minora et al., 2013; Bhambri et al., 2013). However, glaciers in the GHR and Trans  
 460 Himalayan range have been deglaciating with higher average annual rate of 0.4 and  $0.6\% \text{ a}^{-1}$ , respectively during  
 461 the period 1962-2016 (Kulkarni et al., 2007; Kulkarni et al., 2011; Rai et al., 2013; Chand and Sharma, 2015;  
 462 Mir et al., 2017; Schmidt and Nusser, 2017; Chudley et al., 2017; Patel et al., 2018; Das and Sharma, 2018). In  
 463 contrast to these studies, deglaciation rates in SSB, which comprises of glaciers in GHR as well as LR have  
 464 varied from  $0.1\% \text{ a}^{-1}$  (GHR) to  $0.2\% \text{ a}^{-1}$  (LR) (present study). These results evidently depict that the response of  
 465 the SSB glaciers is transitional between the Karakoram Himalayan and GHR glaciers. Period wise area loss of  
 466 the glaciers in the Himalayan region suggest maximum average deglaciation of eastern ( $0.49\%/ \text{yr}$ ), followed by  
 467 central ( $0.36\%/ \text{yr}$ ) and western ( $0.35\%/ \text{yr}$ ) Himalayan glaciers before 2000. Contrarily, after 2000, the central  
 468 Himalayan glaciers deglaciated at the maximum rate ( $0.52\%/ \text{yr}$ ) followed by western ( $0.46\%/ \text{yr}$ ) and eastern  
 469 ( $0.44\%/ \text{yr}$ ) Himalayan glaciers (Fig.8). Though these rates reflect the possible trend of deglaciation in the  
 470 Himalayan terrain, however, any conclusion drawn would be biased due to insufficient data, particularly in  
 471 eastern and central Himalaya.



472  
 473 Figure 8: Annual rate of percentage area loss of glaciers in three major sections of Himalaya before and after  
 474 2000. Details of the same have been mentioned in Table S3 of Supplementary sheet. Results from the present  
 475 study have been star marked in the western Himalaya.  
 476

477 In this study, we found an overall average retreat rate of  $4.3 \pm 1.02 \text{ ma}^{-1}$  during the period 1971-2017. However,  
 478 the average retreat rates of seven glaciers in the SSB, reported by Kamp et al., (2011) is found to be nearly twice  
 479 ( $24 \text{ ma}^{-1}$ ) of that found in this study ( $10 \text{ ma}^{-1}$ ). The comparatively higher retreat rates in the former might be due  
 480 to the consideration of different time frames. The average retreat rates in other basins of the western Himalaya is  
 481 also found to be higher ( $7.8 \text{ ma}^{-1}$ ) in the Doda valley (Shukla and Qadir, 2016),  $8.4 \text{ ma}^{-1}$  in Liddar valley  
 482 (Murtaza and Romshoo, 2015),  $15.5 \text{ ma}^{-1}$  in the Chandra-Bhaga basin (Pandey and Venkataraman, 2013) and 19

483  $\text{ma}^{-1}$  in the Baspa basin (Mir et al., 2017). These results show lower average retreat rate of the glaciers in the  
 484 SSB as compared to the other studies in the western Himalaya.

485 The observed average retreat rates during 2000-2017 ( $4.6 \pm 1.02 \text{ ma}^{-1}$ ) is found to be nearly twice of that, noted  
 486 during 1971-2000 ( $2 \pm 1.7 \text{ ma}^{-1}$ ). Similar higher retreat rates post 2000 have been reported in the Tista basin  
 487 (Raina, 2009), Doda valley (Shukla and Qadir, 2016), Chandra Bhaga basin (Pandey and Venkataraman, 2013)  
 488 and Zanskar basin (Pandey et al., 2011). However, these studies may not sufficiently draw a generalized picture  
 489 of glacier recession in the Himalayan region.

490

## 491 **5.2 Spatio-temporal variability in the climate data**

492 Climatic fluctuations play a crucial role in understanding glacier variability. In this regard, CRU-TS 4.02 dataset  
 493 helped in delineating the long term fluctuations in the temperature and precipitation records.

### 494 **5.2.1 Basin-wide climate variability**

495 During an entire duration of 116 years, i.e. from 1901-2017, maximum mean annual temperature is observed in  
 496 2016 ( $3.23 \text{ }^\circ\text{C}$ ) and minimum during 1957 ( $-0.51 \text{ }^\circ\text{C}$ ). Mean annual temperature shows an almost uniform trend  
 497 till 1996, with a pronounced rise thereafter till 2005/06 period (Fig. 3a;b;c). The globally averaged combined  
 498 land and ocean surface temperature data of 1983-2012 period are considered as the warmest 30-year period in  
 499 the last 1400 years (IPCC, 2013). This unprecedented rate of warming primarily attributed to the rapid scale of  
 500 industrialization, increase in regional population and anthropogenic activities prevalent during this time period  
 501 (Bajracharya et al., 2008; IPCC, 2013). Thus, one of the probable reason for this sudden increase in temperature  
 502 pattern is possibly due to the greenhouse effect from enhanced emission of black carbon in this region (by 61%)  
 503 from 1991-2001. Evidences of incessant increase in temperature during 1990s has also been observed (through  
 504 chronology of Himalayan Pine) from the contemporaneous surge in tree growth rate (Singh and Yadav 2000). In  
 505 fact, 50% of the years since 1970 have experienced considerably high solar irradiance and warm phases of  
 506 ENSO, which is possibly one of the reasons for the considerable rise in temperature throughout the Himalaya  
 507 (Shekhar et al., 2017). Maximum mean annual precipitation is noted during 2015 (615 mm) and minimum  
 508 during 1946 (244 mm). However, the mean annual precipitation followed a similar trend till 1946 with an  
 509 increasing thereafter (Fig. 3a;b;c). Besides these general trends in temperature and precipitation, an overall  
 510 absolute increase in the mean annual temperature ( $T_{\text{max}}$  &  $T_{\text{min}}$ ) and precipitation data have been noted as  $0.77$   
 511  $^\circ\text{C}$  ( $0.25 \text{ }^\circ\text{C}$  &  $1.3 \text{ }^\circ\text{C}$ ) and 158 mm, respectively during the period 1901-2017. These observations suggest an  
 512 enhanced increase in  $T_{\text{min}}$  by nearly 5 times as compared to the  $T_{\text{max}}$  alongwith a simultaneous increase in the  
 513 precipitation during the period 1901-2017.

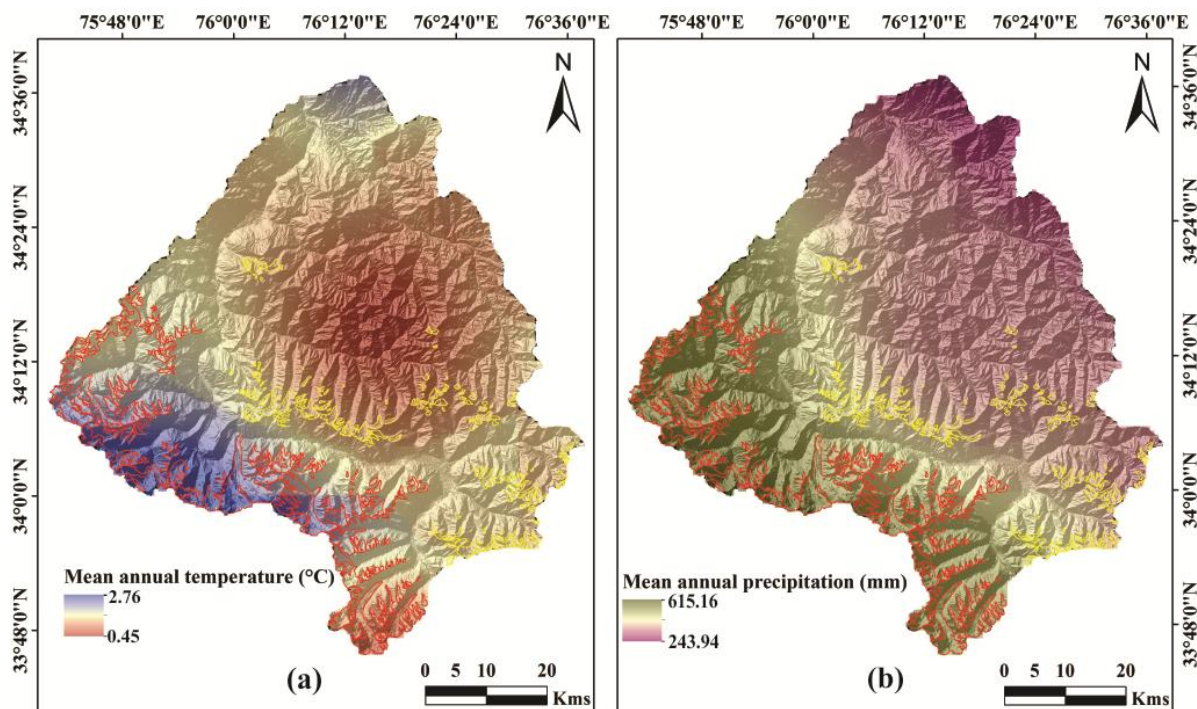
514 Seasonal variations reveal monthly mean temperature and precipitation of  $6.7 \text{ }^\circ\text{C}$  and 1071 mm during summer  
 515 (Apr-Oct) and  $-6.9 \text{ }^\circ\text{C}$  and 890 mm during winter (Nov-Mar) recorded during 1901-2017 period. Maximum  
 516 monthly mean temperature and precipitation have been observed in July ( $11.8 \text{ }^\circ\text{C}/ 50.4 \text{ mm}$ ) and August ( $11.4$   
 517  $^\circ\text{C}/ 52 \text{ mm}$ ) during the period 1901-2017, suggesting them to be the warmest and wettest months. While,  
 518 January is noted to be the coldest ( $-10.4 \text{ }^\circ\text{C}$ ) and November ( $10.3 \text{ mm}$ ) to be the driest months in the duration of  
 519 116 years (Fig. 3d;e;f). Summer/ winter mean annual temperature and precipitation have increased significantly  
 520 by an average  $0.74/ 1.28 \text{ }^\circ\text{C}$  and  $85/ 72 \text{ mm}$ , respectively during the period 1901-2017. These values reveal a  
 521 relatively higher rise in winter average temperature in contrast to the summer. However, enhanced increase in  
 522  $T_{\text{min}}$  ( $1.8^\circ\text{C}$ ) during winter and  $T_{\text{max}}$  ( $0.78^\circ\text{C}$ ) during summer have also been observed during the 1901-2017 time

523 period. The relatively higher rise in the winter temperature (particularly  $T_{\min}$ ) and precipitation possibly suggest  
 524 that the form of precipitation might have changed from solid to liquid during this particular time span. Similar  
 525 increase in the winter temperature have also been reported from the NW Himalaya during the 20<sup>th</sup> century  
 526 (Bhutiyani et al., 2007).

527 In contrast to the long-term climate trends, we have also analyzed the climate data for the study period, i.e.,  
 528 1971-2017. An overall increase in the average temperature ( $0.3^{\circ}\text{C}$ ),  $T_{\max}$  ( $0.45^{\circ}\text{C}$ )  $T_{\min}$  ( $1.02^{\circ}\text{C}$ ) and  
 529 precipitation by 213 mm is observed. Meanwhile, an enhanced increase in winter  $T_{\min}$  ( $1.7^{\circ}\text{C}$ ) and summer  $T_{\max}$   
 530 ( $0.45^{\circ}\text{C}$ ) are observed. These findings aptly indicate the important role of winter  $T_{\min}$  and summer  $T_{\max}$  in the  
 531 SSB.

### 532 5.2.2 Local climate variability

533 Apart from these generalized climatic variations, grid-wise analysis of the meteorological parameters reveal  
 534 existence of local climate variability within the sub-basin (Fig. 3; 9).



535  
 536 Figure 9: Spatial variation in meteorological data recorded for 15 grids in the SSB during the period 1901-2017.  
 537 Map showing the long term mean annual (a) temperature ( $^{\circ}\text{C}$ ) and (b) precipitation (mm) data within the sub-  
 538 basin suggesting the existence of significant local climate variability in the region. Glacier boundaries are shown  
 539 as: GHR (red) and LR (yellow).

540  
 541 Observations indicate that the glaciers covered in grid 4 have been experiencing a warmer climatic regimes with  
 542 the maximum annual mean temperature of  $1.69^{\circ}\text{C}$  as compared to the other glaciers in the region (grid 2 =  $1.4$   
 543  $^{\circ}\text{C}$ , grid 5 =  $0.74^{\circ}\text{C}$ , grid 1 =  $0.65^{\circ}\text{C}$  and grid 3 =  $0.45^{\circ}\text{C}$ ). Spatial variability in annual mean precipitation data  
 544 reveal that grid 2 ( $448\text{ mm}$ ) & grid 1 ( $442\text{ mm}$ ) experienced wetter climate as compared to grid 4 ( $383\text{ mm}$ ),  
 545 grid 3 ( $373\text{ mm}$ ) and minimum in grid 5 ( $318\text{ mm}$ ). These observations suggest that GHR glaciers have been  
 546 experiencing a warmer and wetter climate ( $1.03^{\circ}\text{C}/445\text{ mm}$ ) as compared to the LR glaciers ( $0.96^{\circ}\text{C}/358\text{ mm}$ )

547 (Fig. 3e; f). These observations clearly show that local climate variability does exist in the basin for the entire  
 548 duration of 116 years (Fig. 9).

549

### 550 **5.3 Glacier changes: Impact of climatic and other plausible factors**

551 The alterations in the climatic conditions, discussed in Sect. 5.2, would in turn, influence the glacier parameters,  
 552 however varying with time. This section correlates the climatic and other factors (elevation range, regional  
 553 hypsometry, slope, aspect and proglacial lakes) with the variations in the glacier parameters.

554

#### 555 **5.3.1 Impact of climatic factors**

556 An overall degenerating pattern of the glaciers in the SSB is observed during the period 1971-2017, with  
 557 deglaciation of  $32 \pm 9 \text{ km}^2$  ( $6 \pm 0.02\%$ ). In the same duration, the glaciers have also retreated by an average  $199$   
 558  $\pm 46.9 \text{ m}$  (retreat rate:  $4.3 \pm 1.02 \text{ ma}^{-1}$ ) alongwith an increase in the debris cover by  $\sim 62\%$ . The observed overall  
 559 degeneration of the glaciers have possibly resulted due to the warming of climatic conditions during this  
 560 particular time frame. The conspicuous degeneration of these glaciers might have led to an increased melting of  
 561 the glacier surface, which in turn would have unveiled the englacial debris cover and increased its coverage in  
 562 the ablation zone (Shukla et al., 2009; Scherler et al., 2011). An enhanced degeneration of the glaciers have been  
 563 noted during 2000-2017 ( $0.85 \pm 0.005 \text{ km}^2\text{a}^{-1}$ ) than 1971-2000 ( $0.59 \pm 0.005 \text{ km}^2\text{a}^{-1}$ ). Also, nearly 12 glaciers  
 564 have shown disintegration into glacierets after 2000. These observations may be attributed to the relatively  
 565 higher annual mean temperature ( $1.68 \text{ }^\circ\text{C}$ ) during the former as compared to the period 1971-2000 ( $0.89 \text{ }^\circ\text{C}$ ).  
 566 Concomitant to the maximum glacier degeneration during the period 2000-2017, debris cover extent has also  
 567 increased more (24%) as compared to 1971-2000 (16%). The enhanced degeneration of the glaciers during  
 568 2000-2017 might have facilitated an increase in the distribution of supraglacial debris cover. A transition from  
 569 CGs to PDGs has also been noticed which resulted due to increase in the debris cover percentage over nearly 99  
 570 glaciers. The conversion from PDGs to HDGs (39) and from CGs to HDGs (2) has also occurred. Also, most of  
 571 these transitions have occurred during 2000-2017, which confirms the maximum degeneration of the glaciers  
 572 during this particular period.

573 It is observed in our study that smaller glaciers have deglaciated more (4.13%) than the medium (1.08%) and  
 574 larger (1.03%) sized glaciers during the period 1971-2017 (Supplementary figure S2). This result depicts an  
 575 enhanced sensitivity of the smaller glaciers towards the climate change (Bhambri et al., 2011; Basnett et al.,  
 576 2013; Ali et al., 2017). A similar pattern of glacier degeneration is noted during 1971-2000, with smaller  
 577 glaciers deglaciating more (5%) as compared to the medium sized (3%) and larger (1%) ones. However during  
 578 2000-2017, medium glaciers showed slightly greater degeneration (3.9%) as compared to the smaller (3.7%)  
 579 followed by larger ones (1.5%). We have also observed maximum length change for smaller glaciers (8%) in  
 580 comparison to medium (5%) and large glaciers (3%). These results indicate that the snout retreats are commonly  
 581 associated with small and medium sized glaciers (Mayewski et al., 1980).

582 Temporal and spatial variations in SLAs are an indicator of ELAs, which in turn provide direct evidences  
 583 related to the change in climatic conditions (Hanshaw and Bookhagen, 2014). SLAs are amongst the dynamic  
 584 glacier parameters that alters seasonally and annually, indicating their direct dependency towards the climatic  
 585 factors such as temperature and precipitation. In the present study, the mean SLA has gone up by an average  $22$   
 586  $\pm 60 \text{ m}$  during the period 1977-2017. This rise in SLA is synchronous with the increase in mean annual

587 temperature by 0.43°C. Moreover, the maximum rise in SLA during 1994-2000 is contemporaneous with the  
 588 rise of temperature by 0.64 °C during this time period.

589 Further, in order to understand the regional heterogeneity in glacier response within the sub-basin, parameters of  
 590 the GHR and LR glaciers are analyzed separately at four different time periods and correlated with the climatic  
 591 variables. It is found that the LR glaciers have deglaciated more (7.2%) as compared to the GHR glaciers  
 592 (5.9%). Similarly, more debris cover is found to have accumulated over the LR (73%) glaciers as compared to  
 593 the GHR (59%) glaciers during 1971-2017. This result shows that the relatively cleaner (LR) glaciers tend to  
 594 deglacierate more alongwith accumulation of more debris as compared to the debris and partially debris covered  
 595 glaciers (GHR glaciers) (Bolch et al., 2008; Scherler et al., 2011). Moreover, increase in mean annual  
 596 temperature in the LR (0.3°C) is slightly greater than in GHR (0.25°C) during the period 1971-2017, thus  
 597 exhibiting a positive correlation with deglaciation and debris cover distribution in these regions. We also  
 598 observed that the glacier area, length and debris cover extent of the LR glaciers show a good correlation with  
 599 winter  $T_{min}$  and average precipitation as compared to the GHR glaciers (Table 3). This shows that both  
 600 temperature as well as precipitation influence the degeneration of the glaciers and in turn affects the supraglacial  
 601 debris cover. It is believed that winter precipitation has a prime control on accumulation of snow on the glaciers,  
 602 hence acts as an essential determinant of glacier health (Mir et al., 2017). Also, the negative correlation of  
 603 glacier area with precipitation in this study possibly indicate the major role of increased winter temperature and  
 604 precipitation, which might have decreased the accumulation of snow, thereby decreasing the overall glacier area.  
 605 The average SLA for LR glaciers is observed to be higher as compared to the GHR glaciers. However, a  
 606 relatively higher rise in SLA is observed for GHR in contrast to the LR glaciers. Also, the mean SLA of the  
 607 GHR glaciers shows a good positive correlation with summer  $T_{max}$  as compared to the LR glaciers, while a  
 608 negative correlation with precipitation in the respective year (Table 3). Considering these observations, it  
 609 appears that a general rise in SLA can be attributed to regional climatic warming while that of individual SLA  
 610 variation in glaciers may be related to their unique topography (Shukla and Qadir, 2016).

611 From this analysis, it is quite evident that climatic factors directly influence the glacier response. Also, summer  
 612  $T_{max}$  have a stronger control over SLA, while glacier area,length and debris cover are predominantly controlled  
 613 by the winter  $T_{min}$  in the sub-basin.

614

615 Table 3: Coefficients of determination (r) between respective meteorological (temperature and precipitation)  
 616 data and observed glacier parameters in the Greater Himalayan Range (GHR) and Ladakh Range (LR) at 90%  
 617 confidence.  $T_{avg}$ ,  $T_{min}$  and  $T_{max}$  are montly mean, monthly mean minimum, monthly mean maximum  
 618 temperatures and  $P_{pt}$  montly mean precipitation during different point in time (1971,1994, 2000 and 2017)

Major Mountain Ranges	Glacier Parameters	Climate Variables			
		$T_{avg}$	$T_{min}$	$T_{max}$	$P_{pt}$
GHR	Area	-0.826	<b>-0.897</b>	-0.347	-0.670
	Length	-0.908	<b>-0.926</b>	-0.345	-0.719
	Debris cover	0.842	<b>0.847</b>	0.434	0.593
	SLA	0.725	0.209	<b>0.725</b>	-0.315
LR	Area	-0.900	<b>-0.942</b>	-0.568	-0.779
	Length	-0.909	<b>-0.939</b>	-0.569	-0.778
	Debris cover	0.929	<b>0.907</b>	0.595	0.719
	SLA	0.658	0.395	<b>0.658</b>	-0.505

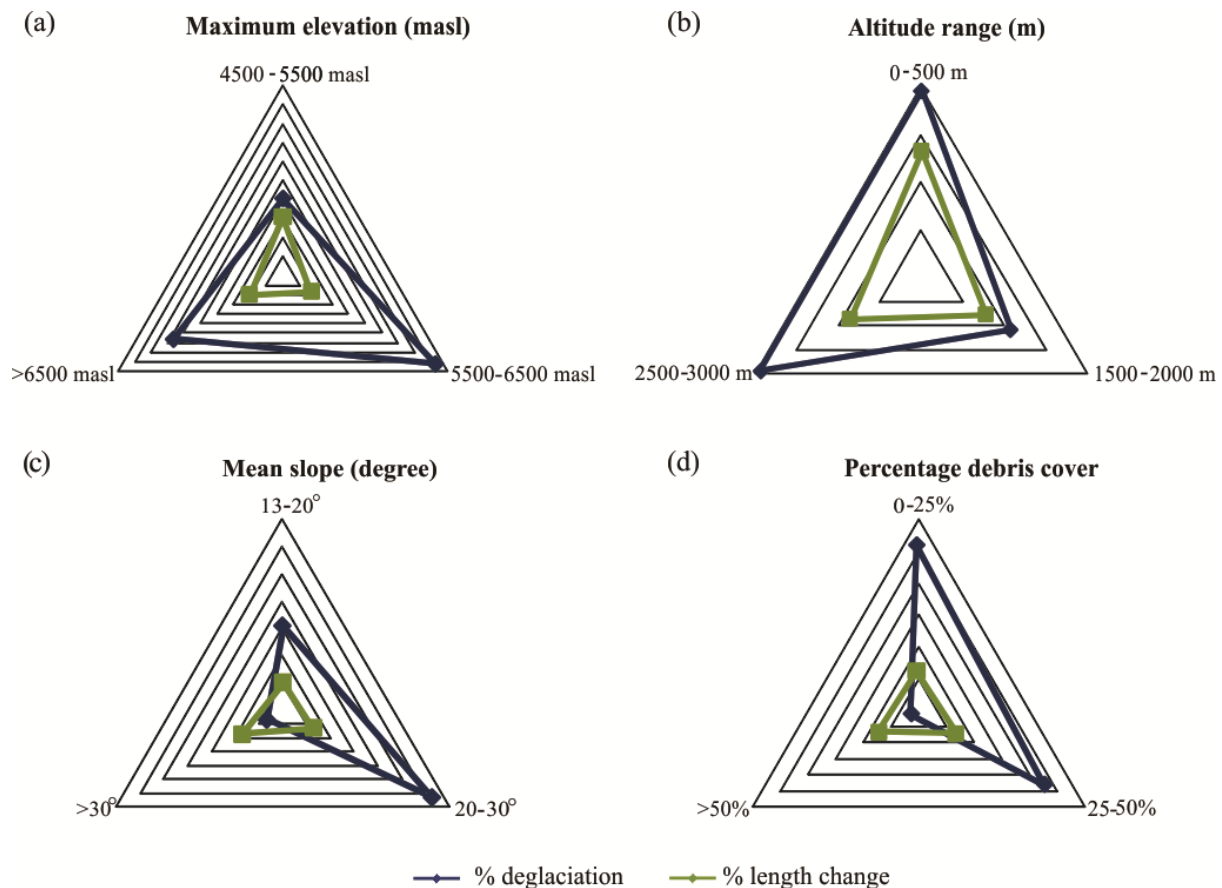
### 619 **5.3.2 Impact of other factors**

620 In addition to the climate variables, other factors such as hypsometry, maximum elevation, altitude range, slope,  
621 aspect and proglacial lakes also influence the response of individual glacier.

622 Glacier hypsometry is a measure of mass distribution over varying altitudes. It is affected by the mean SLA of  
623 the glaciers to a greater extent, as it is considered that if a large portion of the glacier has elevation equivalent to  
624 SLA, then even a slight alteration in SLA might significantly change the ablation and accumulation zones  
625 (Rivera et al., 2011; Garg et al., 2017b).

626 In this study, we observed that GHR and LR glaciers have nearly 45% and 10% of their area at an elevation  
627 similar to SLA. This suggests that GHR glaciers are more susceptible to retreat as compared to the LR glaciers,  
628 as a larger portion of the former belongs to the SLA. Moreover, the hypsometric distribution of glacier area in  
629 the GHR and LR of the SSB reveals maximum area change post 2000 (Fig.6b). In this regard, while GHR  
630 glaciers have undergone relatively higher area loss (21%) at lower elevation (3800-4200 masl), the LR glaciers  
631 lost maximum area (30%) at much higher elevation (5600-5900 masl) ranges (Fig.6b). Besides, a significant  
632 area loss has also been observed for both GHR (6%) and LR (7%) glaciers at their mean elevations post 2000  
633 (Fig.6b).

634 Elevation plays an important role in understanding the accumulation pattern at higher and ablation in the lower  
635 altitudes. The general perception is that the glaciers situated at relatively higher elevation are subjected to  
636 greater amount of precipitation and hence are susceptible to less deglaciation or even mass gain (Pandey and  
637 Venkataraman, 2013). Similarly, we have also noticed that the glaciers extending to comparatively higher  
638 maximum elevation experience minimum retreat (10%) and exhibit higher percentagedeglaciation (33%) as  
639 compared to the glaciers having lower maximum elevation (retreat:15% & deglaciation: 20%) (Fig.10a).



640

641 Figure 10: Differential degeneration of the glaciers during the period 1971-2017 with variability in non-climatic  
 642 factors. (a) Percentage deglaciation and length change of the glaciers at different ranges of maximum elevation,  
 643 (b) altitude range, (c) mean slope and (d) percentage debris cover.

644

645 Moreover, our study shows that the glaciers having lower altitude range have retreated and deglaciated more  
 646 (13% & 20%, respectively) as compared to the counterparts (Fig.10b). These observations indicate that glaciers  
 647 which possess higher maximum elevation and altitudinal range are subjected to less retreat and undergo greater  
 648 deglaciation.

649 Slope is another important factor which has a major role in the sustenance of the glacier as accumulation of ice  
 650 is facilitated by a gentler bedrock topography (DeBeer and Sharp, 2009; Patel et al., 2018). It is observed that  
 651 glaciers having steep slopes (30-40°) have retreated more (17%), however with minimum deglaciation (7%)  
 652 during the period 1971-2017 (Fig.10c). Similar results with steeper glaciers exhibiting minimum deglaciation  
 653 have been reported in the Parbati, Chandra and Miyar basins (Venkatesh et al., 2012; Patel et al., 2018).  
 654 However, it differs with Pandey and Venkataraman (2013) and Garg et al., (2017b), likely due to the differing  
 655 average size:  $25 \pm 33.78$  and  $17 \pm 33.2$  km<sup>2</sup> (present study:  $2 \pm 5.7$  km<sup>2</sup>) and slope: 5-20° and 12-26° (present  
 656 study: 13-41°), respectively, of glaciers used in these studies.

657 Presence of supraglacial debris cover influences the glacier processes. Depending on thickness, debris cover  
 658 may either enhance or retard the ablation process (Scherler et al., 2011). In this study, we observed that clean  
 659 glaciers have undergone maximum deglaciation (52%) as compared to the partially (46%) and heavily debris  
 660 covered glaciers (2%). However, they all have retreated almost similarly (12 to 14%), with slightly higher  
 661 retreat of partially debris covered glaciers (Fig.10d). Aspect/ orientation of glaciers provide information



662 regarding the duration for which they are exposed to the incoming solar radiation. Since, the south facing  
 663 glaciers are subjected to longer duration of exposure to the solar radiations as compared to the north facing  
 664 glaciers, therefore, are prone to greater deglaciation and retreat (Deota et al., 2011). Here, it is observed that the  
 665 glaciers having northerly aspect (north, north-east, north-west) have undergone maximum deglaciation as  
 666 compared to the counterparts. However, majority (71%) of the glaciers have northerly aspect, so any inferences  
 667 drawn in this respect would be biased. It is worthwhile to state that most of the south facing slopes in the basin  
 668 are devoid of glaciers but show presence of relict glacier valleys which would have been glaciated in the past.  
 669 At present only 48 south facing glaciers (south, south-east, south-west) with an average size of  $1 \pm 1.9 \text{ km}^2$  exist  
 670 in the SSB.

671 Similarly, the glacier changes are also influenced by the presence of certain features such as glacial (proglacial  
 672 or supraglacial) lakes or differential distribution of supraglacial debris cover. The presence of a proglacial or  
 673 supraglacial lakes significantly enhances the rate of glacier degeneration by increasing the melting processes  
 674 (Sakai, 2012; Basnett et al., 2013). As per our results, highest average retreat rate ( $\sim 31 \text{ ma}^{-1}$ ) is observed for  
 675 glaciers G-4 (Dulung glacier). Although, it is a debris free glacier, shows the highest retreat rates. Also, a  
 676 moraine-dammed lake is observed at the snout of this glacier and has continuously increased its size from  $0.15$   
 677  $\text{km}^2$  in 1977 to  $0.56 \text{ km}^2$  in 2017. This significant increase in the size of moraine-dammed lake has possibly  
 678 influenced the enhanced retreat rate of the glacier.

## 679 **6 Dataset availability**

680 Temporal inventory data for glaciers of Suru sub-basin, western Himalaya is available at  
 681 <https://doi.pangaea.de/10.1594/PANGAEA.904131> (Shukla et al., 2019).

682

## 683 **7 Conclusions**

684 The major inferences drawn from the study include:

685 1. The sub-basin comprised of 252 glaciers, covering an area of  $481.32 \pm 3.41 \text{ km}^2$  (11% of the glacierized area)  
 686 in 2017. Major disintegration of the glaciers occurred after 2000, with breakdown of 12 glaciers into glacierets.  
 687 Small (47%) and clean (43%) glaciers cover maximum glacierized area of the sub-basin. Topographic  
 688 parameters reveal that majority of the glaciers are north facing and the mean elevation and slope of the glaciers  
 689 are  $5134.8 \pm 225 \text{ masl}$  and  $24.8 \pm 5.8^\circ$ , respectively.

690

691 2. Variability in glacier parameters reveal an overall degeneration of the glaciers during the period 1971-2017,  
 692 with deglaciation of approximately  $0.13 \pm 0.0004\% \text{ a}^{-1}$  alongwith an increase in the debris cover by  $37 \pm 0.002$   
 693  $\text{km}^2$  ( $\sim 62\%$ ). Meanwhile, the glaciers have shown an average retreat rate of nearly  $4.3 \pm 1.02 \text{ ma}^{-1}$  with SLA  
 694 exhibiting an overall rise by an average  $22 \pm 60 \text{ m}$ .

695 3. Long-term meteorological records during the period 1901-2017 exhibit an overall increase in the temperature  
 696 ( $T_{\min}$ :  $1.3^\circ\text{C}$ ,  $T_{\max}$ :  $0.25^\circ\text{C}$ ,  $T_{\text{avg}}$ :  $0.77^\circ\text{C}$ ) and precipitation (158 mm) trends. Both temperature and precipitation  
 697 gradients influence the changes in glacier parameters, however, winter  $T_{\min}$  strongly influencing the glacier area,  
 698 length and debris cover while summer  $T_{\max}$  controlling the SLA. Spatial patterns in change of climate

699 parameters reveal existence of local climate variability in the sub-basin, with progressively warmer (1.03°C) and  
700 wetter (445 mm) climatic regime for glaciers hosted in the GHR as compared to the LR (0.96°C/ 358 mm).

701 4. The inherent local climate variability in the sub-basin has influenced the behavior of the glaciers in the GHR  
702 and LR. It has been observed that LR glaciers have been shrinking faster (area loss: 7%) and accumulating more  
703 debris cover (debris increase: 73%) as compared to the GHR glaciers (6% and 59%) during the period 1971-  
704 2017. The GHR glaciers have, however, experienced greater rise in SLA ( $220 \pm 121$  m) in comparison to the LR  
705 ones ( $91 \pm 56$  m) during the period 1977-2000, with a decrease thereafter.

706

707 Results presented here show the transitional response of the glaciers in the SSB between the Karakoram  
708 Himalayan and GHR glaciers. The study also confirm the possible influence of factors other than climate such  
709 as glacier size, regional hypsometry, elevation range, slope, aspect and presence of proglacial lakes in the  
710 observed heterogenous response of the glaciers. Therefore, these factors need to be accounted for in more details  
711 in future for complete understanding of the observed glacier changes and response.

712

### 713 **Team list**

714 1. Aparna Shukla

715 2. Siddhi Garg

716 3. Manish Mehta

717 4. Vinit Kumar

718 5. Uma Kant Shukla

719

### 720 **Author contribution**

721 A.S. and S.G. conceived the idea and led the writing of manuscript. A.S. structured the study. S.G. performed  
722 the temporal analysis of the data. M.M. and V.K. helped in the field investigation of the glaciers. All the authors  
723 helped in interpretation of results and contributed towards the final form of the manuscript.

724

### 725 **Competing interests**

726 The authors declare that they have no conflict of interest.

727

### 728 **Acknowledgements**

729 Authors are grateful to the Director, Wadia Institute of Himalayan Geology, Dehradun for providing all the  
730 research facilities and support for successful completion of this work. We wish to convey our sincere thanks to  
731 the anonymous reviewers for detailed reviews and constructive comments, which greatly helped to improve the  
732 previous version of the manuscript. We are thankful to Prasad Gogineni (Handling Topical Editor) and Jens  
733 Klump (Handling Chief Editor) for their thoughtful suggestions on the manuscript. Also, we appreciate the  
734 efforts of the entire Editorial team of Earth System Science Data (ESSD) for timely processing of the article.  
735 Aparna Shukla acknowledges the Secretary, Ministry of Earth Science (MoES), New Delhi, India, for providing  
736 requisit support.

737

### 738 **References**

- 739 Ali, I., Shukla, A. and Romshoo, S. A.: Assessing linkages between spatial facies changes and dimensional  
740 variations of glaciers in the upper Indus Basin, western Himalaya, *Geomorphology*, 284, 115-129,  
741 <https://doi.org/10.1016/j.geomorph.2017.01.005>, 2017.
- 742 ALOS Global Digital Surface Model "ALOS World 3D - 30m" (AW3D30).  
743 <http://www.eorc.jaxa.jp/ALOS/en/aw3d30/> (accessed on 1 August 2017).
- 744 Azam, M. F., Wagnon, P., Berthier, E., Vincent, C., Fujita, K. and Kargel, J. F.: Review of the status and mass  
745 changes of Himalayan-Karakoram glaciers, *Journal of Glaciology*, 64, 61-74,  
746 <https://doi.org/10.1017/jog.2017.86>, 2018.
- 747 Bajracharya, S. R., Maharjan, S. B., and Shrestha, F.: The status and decadal change of glaciers in Bhutan from  
748 1980's to 2010 based on the satellite data, *Annals of Glaciology*, 55, 159–166,  
749 <https://doi.org/10.3189/2014AoG66A125>, 2014.
- 750 Bajracharya, S. R., Mool, P. K., Shrestha, B. R.: Global climate change and melting of Himalayan glaciers.  
751 Melting glaciers and rising sea levels: Impacts and implications, Prabha Shastri Ranade (ed), The  
752 Icfai's University Press, India, 28–46, 2008.
- 753 Basnett, S., Kulkarni, A.V. and Bolch, T.: The influence of debris cover and glacial lakes on the recession of  
754 glaciers in Sikkim Himalaya, India, *Journal of Glaciology*, 59, 1035-1046,  
755 <https://doi.org/10.3189/2013JoG12J184>, 2013.
- 756 Bhambri, R., Bolch, T., Chaujar, R. K., and Kulshreshtha, S. C.: Glacier changes in the Garhwal Himalaya,  
757 India, from 1968 to 2006 based on remote sensing, *Journal of Glaciology*, 57, 543–556,  
758 <https://doi.org/10.3189/002214311796905604>, 2011.
- 759 Bhambri, R., Bolch, T. and Chaujar, R. K.: Frontal recession of Gangotri Glacier, Garhwal Himalayas, from  
760 1965 to 2006, measured through high-resolution remote sensing data, *Current Science*, 102, 489–494,  
761 2012.
- 762 Bhambri, R., Bolch, T., Kawishwar, P., Dobhal, D. P., Srivastava, D. and Pratap, B.: Heterogeneity in Glacier  
763 Response in the Upper Shyok Valley, Northeast Karakoram, *The Cryosphere*, 7, 1385–1398.  
764 <https://doi.org/10.5194/tc-7-1385-2013>, 2013.
- 765 Bhattacharya, A., Bolch, Mukherjee, K., Pieczonka, T., Kropacek, J. and Buchroithner, M.: Overall recession  
766 and mass budget of Gangotri Glacier, Garhwal Himalayas, from 1965 to 2015 using remote sensing  
767 data, *Journal of Glaciology*, 62, 1115-1133, <https://doi.org/10.1017/jog.2016.96>, 2016.
- 768 Bhushan, S., Syed, T. H., Arendt, A. A., Kulkarni, A. V. and Sinha, D.: Assessing controls on mass budget and  
769 surface velocity variations of glaciers in Western Himalaya, *Scientific Reports*, 8, 8885,  
770 <https://doi.org/10.1038/s41598-018-27014-y>, 2018.
- 771 Bhutiyani, M. R., Kale, V. S. and Pawar, N. J.: Long term trends in maximum, minimum and mean annual air  
772 temperature across the Northwestern Himalaya during the twentieth century, *Climate change*, 85, 159-  
773 177, <https://doi.org/10.1007/s10584-006-9196-1>, 2007.
- 774 Birajdar, F., Venkataraman, G., Bahuguna, I. and Samant, H.: A revised glacier inventory of Bhaga Basin  
775 Himachal Pradesh, India: current status and recent glacier variations, *ISPRS Annals of*  
776 *Photogrammetry, Remote Sensing and Spatial Information Sciences*, II-8, 37-43, <https://doi.org/10.5194/isprsannals-ii-8-37-2014>, 2014.
- 778 Bolch, T., Buchroithner, M., Pieczonka, T. and Kunert, A.: Planimetric and Volumetric Glacier Changes in the  
779 Khumbu Himal, Nepal, Since 1962 Using Corona, Landsat TM and ASTER Data, *Journal of*  
780 *Glaciology*, 54, 592–600, <https://doi.org/10.3189/002214308786570782>, 2008.
- 781 Bolch, T., Kulkarni, A., Kääb, A., Huggel, C., Paul, F., Cogley, J. G., Frey, H., Kargel, J. S., Fujita, K., Scheel,  
782 M., Bajracharya, S., and Stoffel, M.: The State and Fate of Himalayan Glaciers, *Science*, 336, 310–314,  
783 <https://doi.org/10.1126/science.1215828>, 2012.
- 784 Brun, F., Berthier, E., Wagnon, P., Kääb, A. and Treichler, D.: A spatially resolved estimate of High Mountain  
785 Asia glacier mass balances from 2000 to 2006, *Nature Geoscience*, 10, 668-673, [10.1038/NGEO2999](https://doi.org/10.1038/NGEO2999),  
786 2017.

- 787 Chand, P. and Sharma, M. C.: Glacier changes in Ravi basin, North-Western Himalaya (India) during the last  
788 four decades (1971-2010/13), *Global and Planetary change*, 135, 133-  
789 147, <https://doi.org/10.1016/j.gloplacha.2015.10.013>, 2015.
- 790 Chevuturi, A., Dimri, A. P. and Thayyen, R. J.: Climate change over Leh, Ladakh (India), *Theoretical and*  
791 *Applied Climatology*, 131, 531-545, <https://doi.org/10.1007/s0070401619891>, 2018.
- 792 Chudley, T. R., Miles, E. S. and Willis, I. C.: Glacier characteristics and retreat between 1991 and 2014 in the  
793 Ladakh Range, Jammu and Kashmir, *Remote Sensing Letters*, 8, 518-527,  
794 <https://doi.org/10.1080/2150704X.2017.1295480>, 2017.
- 795 Cogley, J. G.: Glacier shrinkage across High Mountain Asia, *Annals of Glaciology*, 57, 41-49,  
796 <https://doi.org/10.3189/2016AoG71A040>, 2016.
- 797 Das, S. and Sharma, M. C.: Glacier changes between 1971 and 2016 in the Jankar Chhu Watershed, Lahaul  
798 Himalaya, India, *Journal of glaciology*, 1-16, <https://doi.org/10.1017/jog.2018.77>, 2018.
- 799 DeBeer, C. M. and Sharp, M. J.: Topographic influences on recent changes of very small glaciers in the  
800 Monashee mountains, British Columbia, Canada, *Journal of Glaciology*, 55, 691-700,  
801 <https://doi.org/10.3189/002214309789470851>, 2009.
- 802 Deota, B. S., Trivedi, Y. N., Kulkarni, A. V., Bahuguna, I. M. and Rathore, B. P.: RS and GIS in mapping of  
803 geomorphic records and understanding the local controls of glacial retreat from the Baspa Valley,  
804 Himachal Pradesh, India, *Current Science*, 100, 1555–1563, 2011.
- 805 Dimri, A. P.: Interseasonal oscillation associated with the Indian winter monsoon, *Journal of geophysical*  
806 *research: Atmospheres*, 118, 1189-1198, <https://doi.org/10.1002/jgrd.50144>, 2013.
- 807 Dobhal, D. P., Mehta, M. and Srivastava, D.: Influence of debris cover on terminus retreat and mass changes of  
808 Chorabari Glacier, Garhwal region, central Himalaya, India, *Journal of Glaciology*, 59, 961–971,  
809 <https://doi.org/10.3189/2013jog12j180>, 2013.
- 810 Gardelle, J., Berthier, E., Arnaud, Y. and Käab, A.: Region-wide glacier mass balances over the Pamir-  
811 Karakoram-Himalaya during 1999–2011, *The Cryosphere*, 7, 1263–1286, 2013.
- 812 Garg, P. K., Shukla, A., Tiwari, R. K. and Jasrotia, A. S.: Assessing the status of glaciers in parts of the Chandra  
813 basin, Himachal Himalaya: A multiparametric approach, *Geomorphology*, 284, 99-114,  
814 <https://doi.org/10.1016/j.geomorph.2016.10.022>, 2017a.
- 815 Garg, P. K., Shukla, A. and Jasrotia, A. S.: Influence of topography on glacier changes in the central Himalaya,  
816 India, *Global and Planetary change*, 155, 196-212, <https://doi.org/10.1016/j.gloplacha.2017.07.007>, 2017b.
- 818 Garg, S., Shukla, A., Mehta, M., Kumar, V., Samuel, S. A., Bartarya, S. and Shukla, U. K.: Field evidences  
819 showing rapid frontal degeneration of the Kangriz glacier, Suru basin, Jammu and Kashmir. *Journal of*  
820 *mountain science*, 15, 1199–1208, <https://doi.org/10.1007/s11629-017-4809-x>, 2018.
- 821 Garg, S., Shukla, A., Mehta, M., Kumar, V. and Shukla, U. K.: On geomorphic manifestations and glaciation  
822 history of the Kangriz glacier, western Himalaya. *Himalayan Geology*, 40, 115–127, 2019.
- 823 Granshaw, F. D. and Fountain, A. G.: Glacier change (1958– 1998) in the North Cascades National Park  
824 Complex, Washington, USA, *Journal of Glaciology*, 52, 251–256  
825 <https://doi.org/10.3189/172756506781828782>, 2006.
- 826 Guo, Z., Wang, N., Kehrwald, N. M., Mao, R., Wua, H., Wu, Y. and Jiang, X.: Temporal and spatial changes  
827 in western Himalayan firn line altitudes from 1998 to 2009, *Global and Planetary Change*, 118, 97–  
828 105, <https://doi.org/10.1016/j.gloplacha.2014.03.012>, 2014.

- 829 Hall, D. K., Bayr, K. J., Schöner, W., Bindschadler, R. A. and Chiene, J. Y. L.: Consideration of the Errors  
830 Inherent in Mapping Historical Glacier Positions in Austria from the Ground and Space (1893–2001),  
831 Remote Sensing of Environment, 86, 566–577, [https://doi.org/10.1016/S0034-4257\(03\)00134-2](https://doi.org/10.1016/S0034-4257(03)00134-2), 2003.
- 832 Hanshaw, M. N., and Bookhagen, B.: Glacial Areas, Lake Areas, and Snow Lines from 1975 to 2012:  
833 Status of the Cordillera Vilcanota, Including the Quelccaya Ice Cap, Northern Central Andes, Peru,  
834 The Cryosphere, 8, 359–376, <https://doi.org/10.5194/tc-8-359> 2014, 2014.
- 835 Harris, I.C. and Jones, P.D.: CRU TS 4.02: Climatic Research Unit (CRU) year-by-year variation of selected  
836 climate variables by country (CY) version 4.02 (Jan. 1901 - Dec. 2017). Centre for Environmental  
837 Data Analysis, <http://dx.doi.org/10.5285/d4e823f0172947c5ae6e6b265656c273>, 2018.
- 838 India Meteorological Department (IMD), Climatological table: Available online:  
839 [http://www.imd.gov.in/pages/city\\_weather\\_show.php](http://www.imd.gov.in/pages/city_weather_show.php), 2015.
- 840 Immerzeel, W. W., Beek, L. P. H. and Bierkens M. F. P.: Climate change will affect the Asian water towers,  
841 Science, 328, 1382–1385, <https://doi.org/10.1126/science.1183188>, 2010.
- 842 IPCC. Summary for policymakers. In: Stocker, T. F. et al. (Eds), Climate Change 2013: The Physical Science  
843 Basis. Contribution of Working Group III to the Fifth Assessment Report of Intergovernmental Panel  
844 on Climate Change. Cambridge University Press, Cambridge and New York, 2013.
- 845 Kääb, A., Berthier, E., Nuth, C., Gardelle, J. and Arnaud, Y.: Contrasting patterns of early twenty first century  
846 glacier mass change in the Himalayas, Nature, 488, 495–498, <https://doi.org/10.1038/nature11324>,  
847 2012.
- 848 Kääb, A., Treichler, D., Nuth, C., and Berthier, E.: Brief Communication: Contending estimates of 2003–  
849 2008 glacier mass balance over the Pamir–Karakoram–Himalaya, The Cryosphere, 9, 557–564,  
850 <https://doi.org/10.5194/tc-9-557-2015>, 2015.
- 851 Kamp, U., Byrne, M. and Bolch, T.: Glacier Fluctuations between 1975 and 2008 in the Greater  
852 Himalaya Range of Zaskar, Southern Ladakh, Journal of Mountain Sciences, 8, 374–389,  
853 <https://doi.org/10.1007/s11629-011-2007-9>, 2011.
- 854 Kaser, G., Großhauser, M. and Marzeion, B: Contribution potential of glaciers to water availability in different  
855 climate regimes, Proceedings of National academy of Sciences of the United States of America, 107,  
856 20223–20227, <https://doi.org/10.1073/pnas.1008162107>, 2010.
- 857 Kulkarni, A. V., Bahuguna, I. M., Rathore, B. P., Singh, S. K., Randhawa, S. S., Sood, R. K. and Dhar, S.:  
858 Glacial retreat in Himalaya using remote sensing satellite data, Current Science, 92, 69–  
859 74, <https://doi.org/10.1117/12.694004>, 2007.
- 860 Kulkarni, A. V., Rathore, B. P., Singh, S. K. and Bahuguna, I. M.: Understanding changes in Himalayan  
861 Cryosphere using remote sensing technique, International Journal of Remote Sensing, 32,  
862 601–615, <https://doi.org/10.1080/01431161.2010.517802>, 2011.
- 863 Maurer, J. M., Schaefer, J. M., Rupper, S., Corley, A.: Acceleration of ice loss across the Himalayas over the  
864 past 40 years, Science Advances, 5, 1–12 <https://doi.org/10.1126/sciadv.aav7266>, 2019.
- 865 Mayewski, P. A., and Jeschke, P. A.: Himalayan and Trans-Himalayan Glacier Fluctuations Since A.D. 1812,  
866 Arctic and Alpine Research, 11, 267–287, <https://doi.org/>, 1980.
- 867 Miller, J. D., Immerzeel, W. W. and Rees, G.: Climate change impacts on glacier hydrology and river discharge  
868 in the Hindu Kush- Himalaya, Mountain research and development, 32, 461–467,  
869 <http://doi.org/10.1659/MRD-JOURNAL-D-12-00027.1>, 2012.
- 870 Mir, R. A., Jain, S. K., Jain, Thayyen, R. J. and Saraf, A. K.: Assessment of recent glacier changes and its  
871 controlling factors from 1976 to 2011 in Baspa Basin, western Himalaya, Arctic, Antarctic, and Alpine  
872 Research, 49, 621–647, <https://doi.org/10.1657/AAAR0015-070>, 2017.
- 873 Mölg, N., Bolch, T., Rastner, P., Strozzi, T. and Paul, F.: A consistent glacier inventory for Karakoram and  
874 Pamir derived from Landsat data: distribution of debris cover and mapping challenges. Earth  
875 System Science Data, 10, 1807–1827, <https://doi.org/10.5194/essd-10-1807-2018>, 2018.

- 876 Murtaza K. O. and Romshoo S. A.: Recent glacier changes in the Kashmir Alpine Himalayas, India, *Geocarto*  
877 *International*, 32, 188-205, <https://doi.org/10.1080/10106049.2015.1132482>, 2015.
- 878 Nuimura, T., Sakai, A., Taniguchi, K., Nagai, H., Lamsal, D., Tsutaki, S., Kozawa, A.,  
879 Hoshina, Y., Takenaka, S., Omiya, S., Tsunematsu, K., Tshering, P. and Fujita, K.: The GAMDAM  
880 glacier inventory: a quality-controlled inventory of Asian glaciers, *The Cryosphere*, 9, 849-864,  
881 <https://doi.org/10.5194/tc-9-849-2015>, 2015.
- 882 Pandey, A., Ghosh, S. and Nathawat, M. S.: Evaluating patterns of temporal glacier changes in Greater  
883 Himalayan Range, Jammu & Kashmir, India, *Geocarto International*, 26, 321-338,  
884 <https://doi.org/10.1080/10106049.2011.554611>, 2011.
- 885 Pandey, P. and Venkataraman, G.: Changes in the glaciers of Chandra–Bhaga basin, Himachal Himalaya, India,  
886 between 1980 and 2010 measured using remote sensing, *International Journal of Remote Sensing*, 34,  
887 5584-5597, <https://doi.org/10.1080/01431161.2013.793464>, 2013.
- 888 Patel, L. K., Sharma, P., Fathima, T. N. and Thamban, M.: Geospatial observations of topographical control  
889 over the glacier retreat, Miyar basin, western Himalaya, India, *Environmental Earth Sciences*, 77, 190,  
890 <https://doi.org/10.1007/s12665-018-7379-5>, 2018.
- 891 Paul, F., Barrant, N.E., Baumann, S., Berthier, E., Bolch, T., Casey, K., Frey, H., Joshi, S.P., Konovalov, V.,  
892 Bris, R.L. and Mölg, N.: On the accuracy of glacier outlines derived from remote-sensing data, *Annals*  
893 *of Glaciology*, 54, 171–182, <https://doi.org/10.3189/2013AoG63A296>, 2013.
- 894 Paul, F., Bolch, T., Kääb, A., Nagler, T., Nuth, C., Scharrer, K.: The glaciers climate change initiative:  
895 methods for creating glacier area, elevation change and velocity products *Remote Sensing*  
896 *Environment*, 162, 408-426, <http://dx.doi.org/10.1016/j.rse.2013.07.043>, 2015.
- 897 Paul, F., Bolch, T., Briggs, K., Kääb, A., McMillan, M., McNabb, R., Nagler, T., Nuth, C., Rastner, P., Strozzi,  
898 T. and Wuite, J.: Error sources and guidelines for quality assessment of glacier area, elevation change,  
899 and velocity products derived from satellite data in the Glaciers\_cci project, *Remote sensing of*  
900 *Environment*, 203, 256-275, <https://doi.org/10.1016/j.rse.2017.08.038>, 2017.
- 901 Pfeffer, W. T., Arendt, A., Bliss, A., Bolch, T., Cogley, J. G., Gardner, A. S., Hagen, J. O., Hock, R., Kaser, G.,  
902 Kienholz, C., Miles, E. S., Moholdt, G., Molg, N., Paul, F., Radic, V., Rastner, P., Raup, B. H., Rich, J.  
903 and Sharp, M.: The Randolph Glacier Inventory: A globally complete inventory of glaciers, *Journal of*  
904 *Glaciology*, 60, 537-552. doi:10.3189/2014JoG13J176, 2014.
- 905 Pritchard, H. D.: Asia's glaciers are a regionally important buffer against drought, *Nature*, 545, 169-187,  
906 doi:10.1038/nature22062, 2017.
- 907 Racoviteanu, A. E., Arnaud, Y., Williams, M. W. and Ordonez, J.: Decadal changes in glacier parameters in  
908 the Cordillera Blanca, Peru, derived from remote sensing, *Journal of Glaciology*, 54, 499–510,  
909 <https://doi.org/10.3189/002214308785836922,2008a>.
- 910 Racoviteanu, A., Paul, F., Raup, B., Khalsa, S. J. S. and Armstrong, R.: Challenges and recommendations in  
911 mapping of glacier parameters from space: results of the 2008 Global Land Ice Measurements from  
912 Space (GLIMS) workshop, Boulder, Colorado, USA, *Annals of Glaciology*, 50, 53–69,  
913 <https://doi.org/10.3189/172756410790595804>, 2009.
- 914 Rai, P. K., Nathawat, M. S. and Mohan, K.: Glacier retreat in Doda valley, Zaskar basin, Jammu and Kashmir,  
915 India, *Universal Journal of Geoscience*, 1, 139-149, <https://doi.org/10.13189/ujg.2013.010304>, 2013.
- 916 Raina, V. K.: Himalayan glaciers: a state-of-art review of glacial studies, glacial retreat and climate  
917 change. *Himal. Glaciers State-Art Review*, *Glacial Stud. Glacial Retreat Climate Change*, 2009.
- 918 Raina, R. K. and Koul, M. N.: Impact of Climatic Change on Agro-Ecological Zones of the Suru-Zaskar  
919 Valley, Ladakh (Jammu and Kashmir), India, *Journal of Ecology and the Natural Environment* 3,  
920 424–440, 2011.
- 921 Rashid, I., Romshoo, S. A. and Abdullah, T.: The recent deglaciation of Kolahoi Valley in Kashmir Himalaya,  
922 India in response to the changing climate, *Journal of Asian Earth Science*, 138, 38–50,  
923 <https://doi.org/10.1016/j.jseaes.2017.02.002>, 2017.

- 924 Raup, B., Racoviteanu, A., Khals, S. J. S., Helm, C., Armstrong, R., Arnaud, Y.: The GLIMS geospatial glacier  
 925 database: a new tool for studying glacier change, *Global and Planetary Change* 56, 101–110,  
 926 doi:10.1016/j.gloplacha.2006.07.018, 2007.
- 927 Rivera, A., Cawkwell, F., Rada, C. and Bravo, C.: Hypsometry. In: *Encyclopaedia of Snow, Ice and glaciers*,  
 928 Springer, Netherlands, 551-554, 2011.
- 929 Space Application Centre (SAC): Report: Monitoring Snow and Glaciers of Himalayan Region. Space  
 930 Application Centre, ISRO, Ahmedabad, India, 413 pages, ISBN: 978-93-82760-24-5, 2016.
- 931 Sakai, A.: Glacial lakes in the Himalayas: A review on formation and Expansion process, *Global environmental*  
 932 *research*, 23-30, 2012.
- 933 Sakai A. and Fujita, K.: Contrasting glacier responses to recent climate change in high-mountain Asia, *Scientific*  
 934 *reports*, 7, 1-18, <https://doi.org/10.1038/s41598-017-14256-5>, 2017.
- 935 Sangewar, C. V., and S. P. Shukla.: Inventory of the Himalayan Glaciers: A Contribution to the International  
 936 Hydrological Programme, An Updated Edition. Kolkata: Geological Survey of India (Special  
 937 Publication 34), ISSN: 1:0254–0436, 2009.
- 938 Scherler, D., Bookhagen, B. and Strecker, M.R.: Spatially variable response of Himalayan glaciers to climate  
 939 change affected by debris cover, *Nature Geoscience*, 4, 156–159, <https://doi.org/10.1038/ngeo1068>,  
 940 2011.
- 941 Schmidt, S. and Nusser, M.: Changes of High Altitude Glaciers in the Trans-Himalaya of Ladakh over the Past  
 942 Five Decades (1969–2016), *Geosciences*, 7, 27, <https://doi.org/10.3390/geosciences7020027>, 2017.
- 943 Sen, P. K.: Estimates of the regression coefficient based on Kendall's Tau, *American Statistics Journal*, 63,  
 944 1379-1389, <https://doi.org/10.2307/2285891>, 1968.
- 945 Shekhar, M., Bhardwaj, A., Singh, S., Ranhotra, P. S., Bhattacharyya, A., Pal, A. K., Roy, I., Martín-  
 946 Torres, F. J. and Zorzano, M.P.: Himalayan glaciers experienced significant mass loss during later  
 947 phases of little ice age, *Scientific Reports*, 7, 1-14, 2017.
- 948 Shiyin, L., Donghui, S., Junli, Xu., Xin, W., Xiaojun, Y., Zongli, J., Wanqin, G., Anxin, L., Shiqiang, Z.,  
 949 Baisheng, Ye., Zhen, Li., Junfeng, W. and Lizong, W.: Glaciers in China and Their Variations, In:  
 950 Kargel J., Leonard G., Bishop M., Käab A., Raup B. (eds) *Global Land Ice Measurements from Space*,  
 951 Springer Praxis Books, Springer, Berlin, Heidelberg, 2014
- 952 Shukla, A., Gupta, R. P. and Arora, M. K.: Estimation of debris cover and its temporal variation using optical  
 953 satellite sensor data: a case study in Chenab basin, Himalaya, *Journal of Glaciology*, 55, 444-452,  
 954 <http://doi.org/10.3189/002214309788816632>, 2009.
- 955 Shukla, A. and Qadir, J.: Differential response of glaciers with varying debris cover extent: evidence from  
 956 changing glacier parameters, *International Journal of Remote Sensing*, 37, 2453–2479,  
 957 <http://doi.org/10.1080/01431161.2016.1176272>, 2016.
- 958 Shukla, A., Garg, P.K., Manish, M., Kumar, V.: Changes in dynamics of Pensilungpa glacier, western  
 959 Himalaya, over the past two decades, in: *Proceedings of the 38<sup>th</sup> Asian Conference on Remote*  
 960 *Sensing*, Delhi, India, 23-27 October 2017, 2017.
- 961 Shukla, A., Garg, S., Manish, M., Kumar, V and Shukla, U. K.: Temporal inventory of glaciers in the Suru  
 962 sub-basin, western Himalaya, PANGAEA, <https://doi.pangaea.de/10.1594/PANGAEA.904131>, 2019.
- 963 Singh, J. and Yadav, R. R.: Tree-ring indications of recent glacier fluctuations in Gangotri, western Himalaya,  
 964 India, *Current Science*, 79(11), 1598–1601, 2000.
- 965 Vaughan, D. G., Comiso, J. C., Allison, I., Carrasco, J., Kaser, G., Kwok, R., Mote, P., Murray, T., Paul, F.,  
 966 Ren, J., Rignot, E., Solomina, O., Steffen, K. and Zhang, T.: Observations: Cryosphere. in *Climate*  
 967 *change 2013: The physical science basis. Contribution of working group I to the fifth assessment report*  
 968 *of the intergovernmental panel on climate change*, Stocker, T. F., Qin, D., Plattner, G. K., Tignor, M.,  
 969 Allen, S. K., Boschung, J., Nauels, A., Xia, Y., Bex, V. and Midgley, P. M. (Eds.), Cambridge  
 970 University Press, Cambridge, United Kingdom and New York, NY, USA, 2013.
- 971 Venkatesh, T. N., Kulkarni, A. V. and Srinivasan, J.: Relative effect of slope and equilibrium line altitude on the  
 972 retreat of Himalayan glaciers, *The Cryosphere*, 6, 301-311, <http://doi.org/10.5194/tc-6-301-2012>, 2012.

- 973 Vijay, S and Braun, M.: Early 21st century spatially detailed elevation changes of Jammu and Kashmir glaciers  
974 (Karakoram–Himalaya), *Global and Planetary Change*, 165, 137-146,  
975 <http://doi.org/10.1016/j.gloplacha.2018.03.014>, 2018.
- 976 Vittoz, P.: *Ascent of the Nun in the Mountain World: 1954* (Marcel Kurz, ed.), George Allen & Unwin, Ltd.,  
977 London, 1954.
- 978 Zhou, Y., Li, Z., Li, J., Zhao, R. and Ding, X.: Geodetic glacier mass balance (1975-1999) in the central  
979 Pamir using the SRTM DEM and KH-9 imagery, *Journal of Glaciology*, 65, 309-320, doi:  
980 [10.1017/jog.2019.8](https://doi.org/10.1017/jog.2019.8), 2018.